Chapter 2
Characterizing the Structure, Function, and Evolution of Human Solute Carrier (SLC) Transporters Using Computational Approaches

Avner Schlessinger

Abstract Solute Carrier (SLC) transporters are membrane proteins that transport a broad range of solutes including metabolites, ions, toxins, and prescription drugs. In humans, there are about 400 SLC members, many of which are of medical importance. They can be drug target themselves (e.g., the serotonin transporter, SERT) or regulate the absorption, distribution, metabolism, and excretion (ADME) of drugs (e.g., the organic cation transporter 1, OCT-1). An important step toward describing the mechanisms of solute transport by SLC transporters includes computational or experimental characterization of their ligand-bound or unbound structures in different conformations. Due to a variety of technical issues, human SLC transporters are challenging targets for both experimental and computational characterizations. However, recent advances in computational approaches such as molecular docking and comparative modeling, coupled with the atomic structure determination of several membrane transporters, expanded our ability to characterize the human SLC families using in silico structure-based approaches. In this chapter, we first provide an overview of the structure, function, and pharmacology of the human SLC transporters. Second, we describe different computational methods, including sequence analysis, structural modeling, and ligand docking, that are commonly used, in combination with experimental testing, to characterize the human SLC transporters. Third, we demonstrate the utility of these approaches to characterize SLC members with three examples—the norepinephrine transporter (NET), the γ-aminobutyric acid (GABA) transporter 2 (GAT-2), and the L-type amino acid transporter (LAT-1). Finally, future directions in the field of computational structural biology of human SLC transporters are discussed.

A. Schlessinger (✉)
Department of Pharmacology and Systems Therapeutics, Icahn School of Medicine at Mount Sinai, One Gustave L. Levy Place, Box 1603, New York, NY 10029, USA
e-mail: avner.schlessinger@mssm.edu

R. Krämer and C. Ziegler (eds.), *Membrane Transport Mechanism*, Springer Series in Biophysics 17, DOI 10.1007/978-3-642-53839-1_2,

Keywords Comparative modeling • Membrane protein • Molecular docking • Protein function prediction • Structure-based ligand discovery • Virtual screening

2.1 The Human SLC Transporters

2.1.1 Sequences, Structures, and Functions of Human SLC Transporters

The solute carrier (SLC) transporters or the SLC superfamily include membrane transporters, ion channels, and other membrane proteins that mediate the movement of solutes across biological membranes via diverse mechanisms (Hediger et al. 2004; Povey et al. 2001; Saier 2000; Saier et al. 2009; Forrest and Rudnick 2009; Forrest et al. 2011; Jardetzky 1966). In humans, there are about 400 SLC members that are expressed ubiquitously and transport a broad spectrum of molecules, including metabolites, toxins, and drugs (Hediger et al. 2004). For example, the peptide transporter 1 (PepT1, SLC15A1) is a proton-dependent transporter of di and tripeptides that is primarily expressed in the brush border membrane of the intestinal epithelium, where it plays a key role in the uptake of digested proteins and absorption of various peptidomimetic drugs (Smith et al. 2013). Another instance is the γ-aminobutyric acid (GABA) transporter 1 (GAT-1, SLC6A1), an Na^+-dependent transporter localized in the brain's cerebral cortex, where it transports the neurotransmitter GABA at inhibitory synapses, terminating GABA's action and regulating inhibitory postsynaptic signaling (Guastella et al. 1990; Kanner and Zomot 2008). Therefore, genetic variation in SLC members can be associated with various diseases and disorders, and when occurs in transporters that are important for drug absorption, distribution, and excretion (ADME), it can also lead to differential drug response among individuals (pharmacogenetics) (Giacomini et al. 2010). For example, mutations in the organic cation transporter 1 (SLC22A1 or OCT1) affect the intracellular concentrations of the antidiabetic drug metformin (Shu et al. 2003, 2007, 2008; Dresser et al. 2000).

The Gene Nomenclature Committee (HGNC) of the Human Genome Organization (HUGO) defined the human SLC transporters as one "superfamily" (Povey et al. 2001; Hediger et al. 2004). The SLC superfamily is grouped into 52 families based on the number of predicted or observed transmembrane α-helices (TMH; usually 10–14) and sequence similarity, where members of each family typically share sequence identity of 20 % or more to at least one other family member (Hediger et al. 2004). Moreover, some SLC families were classified as such because they are functionally linked to other SLC members. For example, the SLC3 family includes single transmembrane helix proteins that physically interact with members of the SLC7 family of amino acids transporters to form active heterodimers (Verrey et al. 2004). Furthermore, SLC51A and SLC51B, which also function as a heterodimer (similarly to SLC3 and SLC7 families), are grouped into the same family (i.e., SLC51), despite not sharing detectable sequence relationship. Thus, the

use of the term "SLC superfamily," which is commonly used among pharmacologists of membrane transporters (Hediger et al. 2004; Giacomini et al. 2010; Schlessinger et al. 2013b), can be confusing because it generally implies a common ancestor and/or detectable evolutionary relationship, which is not true for the SLC members (Murzin et al. 1995; Saier et al. 2009; Schlessinger et al. 2010, 2013b).

The only human SLC member with experimentally determined atomic resolution structure is the Rhesus glycoprotein ammonium transporter (RhCG, SLC42A3), whose X-ray structure has been determined at resolution of 2.3 Å (Gruswitz et al. 2010). Furthermore, the mouse mitochondrial uncoupling protein 2 UCP2/SLC25A8, which exhibits sequence identity of ~96 % to its human ortholog, has recently been determined via NMR (Berardi et al. 2011). There are several high-resolution structures of proteins from prokaryotic and other eukaryotic organisms that are sufficiently similar in sequence to the human SLC members to inform about their general topology and fold (Gether et al. 2006; Schlessinger et al. 2010, 2013a, b; Faraldo-Gomez and Forrest 2011; Pieper et al. 2013). These structures confirmed that the human SLC transporters are diverse in structure, as was expected from their divergent sequences. A recent analysis suggested that the two largest structural classes or folds in the human SLC members are the Major Facilitator Superfamily (MFS; e.g., GLUTs/SLC2) and the Neurotransmitter: Sodium Symporter (NSS) fold, which is also dubbed the APC (amino acid-polyamine-organoCation) superfamily (Lomize et al. 2006) or the LeuT-like fold (e.g., SLC6) (Schlessinger et al. 2010). Conversely, these atomic structures also revealed that some SLC families are related structurally, despite sharing weak sequence relationships (sequence identity lower than 10 %). For example, the structures of several prokaryotic homologs of the human families SLC5 (the Na^+-glucose co-transporter SGLT) (Faham et al. 2008), SLC6 (the leucine/alanine transporter LeuT) (Yamashita et al. 2005), and SLC7 [arginine/agmatine antiporter (AdiC) (Gao et al. 2009; Fang et al. 2009; Shaffer et al. 2009)], as well as other transporters, such as the uracil transporter UraA (Lu et al. 2011), the Na^+-hydantoin transporter Mhp1 (Weyand et al. 2008), the Na+/betaine symporter BetP (Ressl et al. 2009), the glutamate/gamma-aminobutyrate antiporter (Ma et al. 2012), and the L-carnitine/gamma-butyrobetaine antiporter CaiT (Schulze et al. 2010), all belong to the NSS fold (Schlessinger et al. 2010; Lomize et al. 2006).

The majority of the human SLC members are thought to transport substrates via the "alternating access" transport mechanism, in which the transporter interchangeably exposes its binding site at either side of the membrane (Forrest and Rudnick 2009; Kanner and Zomot 2008; Krishnamurthy et al. 2009; Forrest et al. 2008, 2011; Jardetzky 1966; Guan and Kaback 2006; Krishnamurthy and Gouaux 2012; Abramson and Wright 2009; Perez and Ziegler 2013). The alternating access is highly conserved among secondary active transporters, even among families that are unrelated in sequence and structure, such as proteins of the MFS (see Chaps. 6 and 7), NSS (see Chaps. 3, 4, and 5), and the glutamate transporter folds (see Chap. 1). Importantly, this mechanism is enabled by inverted structural repeats that are highly divergent in sequence (Saier 2000; Forrest et al. 2011; Krishnamurthy

et al. 2009; Abramson and Wright 2009; Khafizov et al. 2010; Yamashita et al. 2005; Madej et al. 2013). For example, LeuT includes two five transmembrane helices repeats that are related to each other via a twofold pseudo-symmetry axis parallel to the membrane plane; the repeats make a channel and the first helix of each repeat coordinates ligand binding (Forrest et al. 2011; Krishnamurthy et al. 2009). The evolution of these pseudo-repeats in the SLC structures and how they contribute to the diverse energy couplings of the transporters are not completely understood and are likely to differ among different families. (Forrest et al. 2008; Forrest and Rudnick 2009; Perez and Ziegler 2013; Yamashita et al. 2005; Khafizov et al. 2010; Madej et al. 2013; Forrest 2013). Recent studies support the notion that the transport mechanism is conserved among members of the NSS fold (Abramson and Wright 2009; Krishnamurthy et al. 2009; Shaffer et al. 2009; Ressl et al. 2009; Shi and Weinstein 2010). For example, using comparative modeling and molecular dynamics simulations, Shi and Weinstein revealed that the positive charge of the a sodium ion (NA2) in LeuT is equivalent to a proton in ApcT (i.e., Lys158) in regulating specific conformational changes that are associated with transport (Shi and Weinstein 2010). Interestingly, a recent analysis of the MFS transporters LacY and FucP suggested that although these transporters share only weak sequence similarities, their structural repeats consist of triple helix units that are related to each other and have likely emerged from a common ancestor (Madej et al. 2013) (see Chap. 6). This suggests a simple, parsimonious chain of events that may have led to the sequence divergence among members of the MFS fold, which might be relevant to other SLC families including those in human.

2.1.2 Description of Substrate Specificity in Human SLC Transporters

The SLC transporter's function is determined by its structure and dynamics. In particular, the shape and physicochemical properties of the binding site(s) on the transporter surface (i.e., specificity determinants) determine the ligands (molecules or ions) that bind to the transporter ("binding specificity determinants"), which contribute to define the ligands that get transported by the transporter ("substrate specificity determinants"); the mechanism of transport describes how the specificity determinants of a transporter result in the binding specificity and substrate specificity. Description of specificity determinants in SLC families includes the characterization (computationally and/or experimentally) of different conformational states that the transporters undergoes during transport and inhibition, as well as the identification of structural relationships between the transporter and its ligands, including inhibitors and substrates.

Understanding these structure–function relationship in the SLC transporters can contribute to three key clinically important aspects of their functions (Schlessinger

et al. 2013b). First, and perhaps obvious, identification of structural relationships in protein–ligand complexes of structurally related transporters can provide molecular basis for how ions and molecules get transported selectively across the membranes of human cells and organelles, which is essential for many of life's processes. For example, charge specificity within the organic ion transporter family SLC22, which is important for drug ADME in the kidney and liver, has been previously proposed based on biochemical data (Feng et al. 2001) and was recently rationalized using comparative models of representative members of the family (Pedersen et al. 2013); it was suggested that the organic anion transporter 3 (OAT3, SLC22A8) binding site residue Arg454, has its charge reversed in the organic cation transporter 1 (OCT1, SLC22A1) (Asp 474), in agreement with the role of the corresponding residue of the template structure in substrate charge specificity (Pedersen et al. 2013).

Second, the functional effect of clinically important genetic variants, including those variants that are associated with disease states or pharmacogenetics, can be rationalized based on their location on the protein structure. For example, the negative effect of variants in the proton-dependent Multidrug and toxin extrusion 2 (MATE2-K, SLC47A2), on the response to the antidiabetic drug metformin, was rationalized by their predicted impact on the MATE2-K comparative model (Choi et al. 2011); Gly393 mutation to arginine occurs in close proximity to the putative proton-binding site and likely affect interaction with cationic ligands and protons.

Third, unknown endogenous (e.g., metabolites) and exogenous (e.g., prescription drugs) ligands can be predicted by virtual screening of large small molecule libraries against the transporter structure. The experimentally validated ligands can then guide drug–drug interaction studies, provide novel chemical probes to characterize the transporter function, and serve as lead-like molecules for drug development. For example, virtual screening against the structural model of the norepinephrine transporter NET, followed experimental testing of top-scoring hits, revealed that several prescription drugs interact with NET. These results rationalize some of the positive and/or negative effects of some of these drugs (Schlessinger et al. 2011).

We begin this book chapter by describing computational tools, including sequence analysis, comparative modeling, model refinement and assessment, and virtual screening, that are commonly used to predict the structures and functions of SLC transporters. We then illustrate the applications of these tools in combination with experiments to define specificity determinants for selected SLC transporters. We conclude by discussing future directions in field.

2.2 Structure-Based Ligand Discovery for SLC Transporters

2.2.1 Overall Approach

In structure-based ligand discovery, a large virtual library of small organic molecules is computationally docked against an atomic structure of a protein target (Shoichet 2004) (Fig. 2.1). For a protein without an experimentally determined structure, virtual screening or molecular docking can be performed against structural model of the target protein (Jacobson and Sali 2004). In general, structural models for proteins can be constructed by using three main approaches. They include (1) comparative or homology modeling, which relies on detectable similarity between the target protein and least one known experimentally determined structure, (2) ab initio modeling, which uses sequence alone, without relying on similarity at the fold level between target protein and experimentally determined structures, and (3) hybrid methods modeling, which combines low-resolution experimental data such as that obtained from electron microscopy of 2D crystals using computational modeling with comparative modeling, ab initio modeling, or both (Baker and Sali 2001; Russel et al. 2012; Rohl et al. 2004). Considerable progress has been made recently in all three modeling categories, particularly for membrane proteins (Yarov-Yarovoy et al. 2006; Marks et al. 2011; Hopf et al. 2012; Nugent and Jones 2012). Notably, ligand discovery with molecular docking requires highly accurate and precise description of the target protein binding site. For example, incorrect configuration of even one side chain in the transporter binding site can yield results similar to that of random prediction (Schlessinger et al. 2011). Therefore, models calculated using comparative modeling are expected to be the most useful for virtual screening.

We take an iterative comparative modeling and ligand docking approach to predict ligands for human SLC transporters. In brief, we begin with a sequence of a transporter with unknown structure ("target") and identify homologous proteins with known structures, using sequence-based alignment and/or fold recognition methods (e.g., Promals3D (Pei et al. 2008)) (Fig. 2.1a). The alignment is corrected manually for different aspects of protein structure and function, including transmembrane helices (TMH), sequence motifs, and experimentally verified conserved residues (Fig. 2.1b). Initial structural models are then built with modeling programs such as MODELLER (Sali and Blundell 1993) and assessed using various statistical potentials that are derived from experimentally determined sequences (e.g., Z-DOPE (Shen and Sali 2006)) (Fig. 2.1c). The models are refined by modeling the loops, repacking the side chains on a fixed backbone, as well as by energy minimization using Molecular Dynamics (MD) simulations (Fig. 2.1d) (Hess et al. 2008; Schlessinger et al. 2012). Next, comparative models are evaluated based on their ability to discriminate known ligands from decoys by using docking against the binding site of the target (i.e., "enrichment calculations") (Fig. 2.1e)

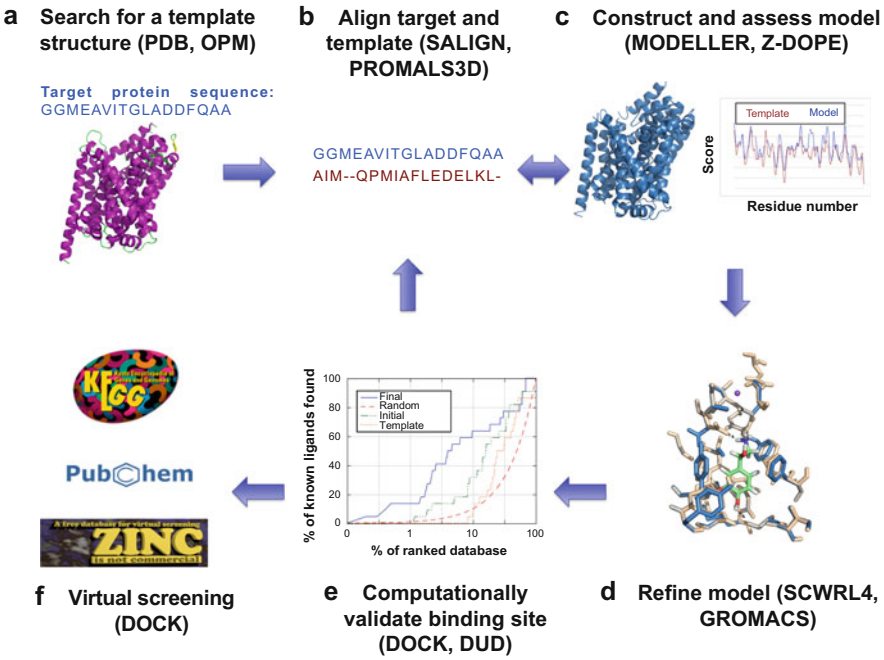

Fig. 2.1 Steps in structure-based ligand prediction

(Huang et al. 2006; Fan et al. 2009; Schlessinger et al. 2011; Lorber and Shoichet 1998). Thus, by selecting models based on their enrichment scores, comparative models are assessed for the utility in predicting ligands. The modeling steps and enrichment calculations can be performed iteratively to optimize the models for virtual screening applications (Evers et al. 2003; Cavasotto et al. 2008; Carlsson et al. 2011; Schlessinger et al. 2012). Virtual screening is then performed where large compound libraries, which can contain millions of purchasable compounds (e.g., ZINC (Irwin and Shoichet 2005)), are docked against the high-ranking models (Fig. 2.1f) (Shoichet 2004; Shoichet et al. 1993). Finally, top-ranked compounds and their orientation relative to the target binding site ("poses") are analyzed manually and selected for experimental validation.

2.2.2 *Template Identification and Target–Template Alignment*

As for other proteins, to construct a comparative model for an SLC transporter target, most similar known template structure or structures need to be detected and aligned with its sequence (Sali and Blundell 1993). The majority of the SLC

families share similar topology (10–14 TMH); thus, a key step toward aligning their sequences optimally involves the accurate identification of these TMH regions (Kernytsky and Rost 2003; Elofsson and von Heijne 2007; Punta et al. 2007; Nugent and Jones 2012). Early TMH prediction methods primarily included "hydropathy plots" derived from "propensity scales," which usually include 20 values corresponding to amino acid properties when found in membrane spanning helices (e.g., the Kyte–Doolite hydrophobicity scale (Kyte and Doolittle 1982)). These methods were shown to be surprisingly accurate because of the compositional bias on the amino acid sequence of membrane proteins imposed by the lipid bilayer environment (Elofsson and von Heijne 2007; Eyre et al. 2004; Punta et al. 2007).

However, state-of-the-art TMH prediction methods, which typically use advanced statistical inference methodologies (e.g., machine-learning algorithms) and usually combine more than one approach, are significantly more accurate than the early TMH prediction methods (i.e., accuracy of 80–90 %) (Punta et al. 2007; Nugent and Jones 2012) (Table 2.1). For example, the support vector machine program MEMSAT-SVM, which was trained on structurally derived topology data and sequence profiles, achieved ~90 % accuracy on a set of experimentally determined membrane protein structures (Nugent and Jones 2009). A recent study comprehensively evaluated the performance of topology prediction methods on various sets including a set of 103 newly determined atomic structures (Tsirigos et al. 2012). This analysis indicated that the best performance is obtained by TOPCONS (Bernsel et al. 2009), a consensus method that combines five other prediction methods (e.g., SCAMPI (Bernsel et al. 2008)) and that the best method for distinguishing membrane from non-membrane proteins is the Hidden Markov Model (HMM)-based method Phobius (Kall et al. 2005).

The identification of the best templates for modeling is relatively straightforward for some human SLC members. In particular, several human SLC families exhibit sequence similarities of 30–40 % to proteins of known structure. For example, the human Na^+-coupled nucleoside transporters (SLC28), the oligopeptide:H^+ co-transporters (SLC15), and the high-affinity glutamate and neutral amino acid transporter family (SLC1) are homologs of the proteins of known structures vcCNT (Johnson et al. 2012), PEPTso (Newstead et al. 2011), and Glt(Ph) (Yernool et al. 2004), respectively. For these families the template identification is feasible even when using relatively simple sequence-based alignment methods such as BLAST (Altschul et al. 1990; Rost et al. 2003).

However, the template identification for other human SLC families and the template–target alignment can be more difficult. Such challenging targets can be transporters that are distantly related to proteins of known structure. For instance, members of the SLC22 family of organic cation/anion/zwitterion transporters share sequence identity of 20 % or lower with the closest template structure—the structure of the fungal phosphate transporter PiPT (Pedersen et al. 2013). Other challenging targets can be those that exhibit significant (yet often distant) sequence similarity to more than one potential template structure. For instance, the SLC7 family of amino acid transporters is related to several transporters with known

Table 2.1 Sequence-based methods

Method[a]	Type[b]	URL[c]	Reference[d]
Transmembrane helix prediction			
MEMSAT-SVM	S, P	http://bioinf.cs.ucl.ac.uk/psipred/	Nugent and Jones (2009)
TOPCONS	S, P	http://topcons.cbr.su.se	Bernsel et al. (2009)
SCAMPI	S	http://scampi.cbr.su.se	Bernsel et al. (2008)
Phobius	S, P	http://phobius.sbc.su.se	Kall et al. (2005)
PHDhtm	S, P	http://www.predictprotein.org	Rost et al. (1995)
TMHMM2	S, P	http://www.cbs.dtu.dk/services/TMHMM	Sonnhammer et al. (1998)
Template detection and alignment			
HHpred	S, P	http://www.toolkit.tuebingen.mpg.de/hhpred	Soding et al. (2005)
MAFFT	S, P	http://www.mafft.cbrc.jp/alignment/server/	Katoh and Toh (2008)
PROMALS3D	S, P	http://prodata.swmed.edu/promals3d/promals3d.php	Pei et al. (2008)
SALIGN	S, P	http://modbase.compbio.ucsf.edu/salign-cgi/index.cgi	Madhusudhan et al. (2009)
AlignMe*	S, P	http://www.bioinfo.mpg.de/AlignMe	Khafizov et al. (2010)
MP-T*	S	http://www.opig.stats.ox.ac.uk/webapps/MPT/php/	Hill and Deane (2013)
PRALINE™*	S	http://www.ibi.vu.nl/programs/pralinewww/	Pirovano et al. (2008)
TM-Coffee*	S	http://www.tcoffee.crg.cat/apps/tcoffee/do:tmcoffee	Chang et al. (2012)

[a]*Method* marks computational sequence-based tools for TMH prediction and template detection/alignment. Template detection and alignment methods specifically designed for membrane proteins are marked with "*"
[b]*Type* gives type of the prediction method; "S" and "P" correspond to a web server and a computer program, respectively
[c]*URL* provides the Internet address for the service
[d]*Reference* gives the primary literature describing the method

structures of the APC family such as the amino acid transporter ApcT from *Methanococcus jannaschii* (Shaffer et al. 2009) and the arginine:agmatine antiporter AdiC from *Escherichia coli* (Gao et al. 2010).

For such challenging targets more state-of-the art fold assignment and threading methods need to be applied and analyzed carefully. They include profile–profile alignment and fold recognition methods that rely on observed or predicted structural information (e.g., HHpred (Soding et al. 2005)), multiple sequence alignment methods (e.g., MAFFT (Katoh and Toh 2008)), as well as methods that combine these approaches (e.g., Promals3D (Pei et al. 2008)). Several alignment methods have been specifically optimized to align membrane proteins (Khafizov et al. 2010; Hill and Deane 2013; Pirovano et al. 2008; Chang et al. 2012) (Table 2.1). Two recent developments include (1) alignment of membrane proteins (AlignMe), which is a user-friendly program that uses information such as residue

hydrophobicity and predicted secondary structure to align sequences or hydropathy profiles of membrane proteins (Khafizov et al. 2010; Stamm et al. 2013) and (2) membrane protein threader (MP-T), which is a sequence-structure alignment method based on multiple sequence alignment (Hill and Deane 2013). MP-T uses predicted and observed information such as accessible surface area, membrane positioning, as well as secondary structure derived from homologs of the target protein. MP-T achieved higher accuracy than other alignment methods (e.g., Promals3D) using a variety of measures. For instance, models based on MP-T alignment were more accurate than those based on the best alternative alignment tool, where 25 % of the test set proteins exhibited an increase of $\geq$4 % in the global distance test total score (GDT_TS), which measures structural similarity between two protein structures with identical amino acid sequences (Zemla et al. 1999; Hill and Deane 2013).

Sequence similarity networks that visualize relationships among protein sequences and structures have shown to be useful in annotating the structures and functions of human SLC transporters (Schlessinger et al. 2010, 2013b). In brief, Schlessinger et al. first performed an "all-against-all" profile–profile comparison with SALIGN (Madhusudhan et al. 2009) among all the human SLC members. In combination with sequence-based clustering, they constructed and visualized sequence-based similarity networks for which varying cutoffs to define related sequences were examined. The final cutoffs, some representing distant sequence relationships (sequence identity of ~15 %), were selected to be permissive enough to detect the majority of known distant relationships among SLC members with minimal false positives. The analysis identified previously unknown relationships among human SLC families. For example, it was predicted that the glucose transporter family (GLUT, SLC2) are related to the organic ion transporter family (SLC22), which was subsequently confirmed experimentally for representative members of these families (Schlessinger et al. 2010). This similarity network also captured the structural similarity among the SLC5, SLC6, and SLC7 families (NSS fold) and predicted that other human families, including the SLC32 (the vesicular inhibitory amino acid transporter family), SLC36 (the proton-coupled amino acid transporter family), and SLC38 (System A and System N sodium-coupled neutral amino acid transporter family) are members of the NSS fold.

Recent discoveries of previously unknown human SLC families (i.e., SLC49-52) and the substantial increase of experimentally determined atomic structures of homologs from various organisms initiated an updated comprehensive analysis of the SLC members (Schlessinger et al. 2013b). For example, it was shown that the SLC52 family of riboflavin transporters is highly connected to the SLC29 of nucleoside transporters, suggesting that they are related in structure, function, or even both.

2.2.3 *Model Construction, Refinement, and Assessment*

Once a template structure or structures have been identified and aligned to the target sequence, an atomic comparative model can be constructed. The underrepresentation of experimentally determined membrane protein structures makes the human SLC targets difficult targets for modeling for two main reasons. First, there is only a small number of closely related protein structures; thus, researchers often rely on templates that are only distantly related to their target proteins (e.g., share the same fold). Second, most modeling methods were not optimized for membrane proteins, therefore, unique structural properties (e.g., specific interhelical interactions (Harrington and Ben-Tal 2009)) are often missed by the current prediction methods. Interestingly, a previous benchmark study revealed that the model accuracy of membrane proteins strongly depends on the sequence similarity between the target and template, similarly to globular proteins (Forrest et al. 2006). For example, comparative models corresponding to the transmembrane regions exhibited <2 Å Cα RMSD to the native structure for targets that share sequence identity of 30 % or more with their templates. Although these results are encouraging, the same study identified the loop regions connecting the transmembrane regions to be considerably less accurate than the transmembrane domains (Forrest et al. 2006).

However, a recent increase in the number of atomic structures of membrane proteins (Pieper et al. 2013), particularly of SLC homologs (Schlessinger et al. 2013b), has expanded our ability to model the structures of many previously unmodelable pharmacologically important SLC transporters, including drug target (e.g., SLC2/GLUTs) and drug ADME (e.g., CNTs) transporter families. Some of these transporters can now be modeled with accuracy that might be sufficient for virtual screening (Schlessinger et al. 2010, 2013b; Pieper et al. 2013). For example, the concentrative nucleoside transporter from *Vibrio cholerae* (vcCNT) (Johnson et al. 2012) structure (resolution of 2.4 Å) was determined in a ligand-bound conformation. vcCNT shares sequence identity of 35–40 % and a highly similar binding site with the human SLC28/CNTs family, whose members transport key anticancer and antiviral drugs, thereby providing an excellent template for modeling of these proteins (Johnson et al. 2012).

Comparative modeling programs typically rely on several common approaches [reviewed in Sanchez and Sali (1998) and Marti-Renom et al. (2000)]. For example, the program MODELLER calculates comparative models based on satisfaction of spatial restraints that are derived from the target–template alignment, atomic statistical potentials, and molecular mechanics (Sali and Blundell 1993) (Table 2.2). MODELLER exists as standalone program and can also be run through the structure analysis and visualization program UCSF CHIMERA (Pettersen et al. 2004) or via the web server ModWeb (Pieper et al. 2011). ModWeb and another highly popular comparative modeling server, Swiss-Model (Kiefer et al. 2009), can take as input protein sequence and perform key steps of comparative modeling automatically, including template identification, target–template alignment, model building,

Table 2.2 Structural modeling methods

Method[a]	Type[b]	URL[c]	Reference[d]
Comparative modeling			
MODELLER/ ModWeb	S, P	http://modbase.compbio.ucsf.edu/ModWeb20-html/modweb.html	Sali and Blundell (1993)
Swiss-Model	S, P	http://swissmodel.expasy.org/	Kiefer et al. (2009)
MEDELLER*	S	http://opig.stats.ox.ac.uk/webapps/medeller/home.pl?app=MEDELLER	Kelm et al. (2010)
Model assessment			
ModEval	S, P	http://modbase.compbio.ucsf.edu/modeval/help.cgi?type=help	Eramian et al. (2008)
Verify3D	S, P	http://nihserver.mbi.ucla.edu/Verify_3D/	Bowie et al. (1991)
PROCHECK	S, P	http://nihserver.mbi.ucla.edu/SAVES/	Laskowski et al. (1993)
Model refinement			
ModLoop	S, P	http://www.modbase.compbio.ucsf.edu/modloop/	Fiser and Sali (2003)
ArchPRED	S	http://manaslu.aecom.yu.edu/loopred/	Fernandez-Fuentes et al. (2006)
LoopyMod	P	http://wiki.c2b2.columbia.edu/honiglab_public/index.php/Software:Loopy	Soto et al. (2008)
RosettaMembane*	S, P	https://www.rosettacommons.org/software/	Yarov-Yarovoy et al. (2006)
GROMACS*	P	http://www.gromacs.org/	Hess et al. (2008)
Positioning in the membranous environment			
iMEMBRANE	S	http://opig.stats.ox.ac.uk/webapps/medeller/home.pl?app=iMembrane	Kelm et al. (2009)
PPM	S	http://opm.phar.umich.edu/server.php	Lomize et al. (2012)
TMDET	S	http://tmdet.enzim.hu/?go=form	Tusnady et al. (2005)

[a]*Method* marks freely available methods for model construction, assessment, analysis, and refinement. Comparative modeling and model refinement methods specifically optimized for membrane proteins are marked with "*"
[b]*Type* gives type of the prediction method; "S" and "P" correspond to a web server and computer program, respectively
[c]*URL* provides the Internet address for the service
[d]*Reference* gives the primary literature describing the method

and model assessment. Moreover, several recent programs have been designed to model the structures of membrane proteins (Kelm et al. 2010; Yarov-Yarovoy et al. 2006). For example, MEDELLER works by first identifying a reliable core structure and subsequently building a structural model by extending the core to other transmembrane regions and loops (Kelm et al. 2010). MEDELLER performance is overall better than that of MODELLER for membrane protein targets; however, for targets that share 20–40 % with their templates (i.e., "medium" set), which is the case for most of the modelable human SLC targets (Schlessinger et al. 2010, 2013b), MODELLER is slightly more accurate (RMSD of 5.33 vs 5.84 Å for MEDELLER) (Kelm et al. 2010).

After an initial model has been built, the model can be further refined. In particular, loop modeling, which usually does not require a template structure, can be employed for the non-membranous loop regions that connect the transmembrane helices; several top-performing loop modeling methods are publically available as downloadable programs (e.g., LoopyMod (Soto et al. 2008), PLOP (Jacobson et al. 2004)), via a web server (e.g., ArchPRED (Fernandez-Fuentes et al. 2006)), or both (ModLoop (Fiser and Sali 2003)). In addition, comparative models can be further refined by optimized the sidechain configuration on a fixed backbone conformation (Krivov et al. 2009; Xiang et al. 2007). For example, the program SCWRL4 is based on a graph theory algorithm that solves the combinatorial problem in side chain prediction faster than other approaches (Krivov et al. 2009). Finally, MD simulations (e.g., with GROMACS (Hess et al. 2008)) can be employed to minimize the energy of models thus refining the initial model, where an implicit solvent model can be used to account for the hydrophobic membrane environment (Lindorff-Larsen et al. 2010; Shaw et al. 2010) (Table 2.2).

Evaluation of the model accuracy is important for its appropriate interpretation. For example, the sequence identity between the target and template is related to the model accuracy, where models that share sequence identity of 50 % or more with their templates are expected to have 1 Å root mean square (RMS) error for the main chain atoms, making them potentially suitable for ligand docking (Baker and Sali 2001). Because the sequence identity is a crude measure that is not correlated strongly with model, various advanced methods have been developed for evaluation comparative models (Marti-Renom et al. 2000; Eramian et al. 2008). Perhaps the most popular model evaluation approaches are knowledge-based statistical potentials that are derived from distributions of structural features in experimentally determined protein structures (Melo et al. 2002). For instance, Z-DOPE is an atomic distance-dependent statistical potential that is implemented in MODELLER (Shen and Sali 2006); ModEval is a server that evaluates the accuracy of models using a variety of statistical potentials and a support vector machine predicting the accuracy of the model based on nine features, such as sequence similarity measures and statistical potentials that are extracted from a tailored training set of models unique to the assessed model (Eramian et al. 2008). Furthermore, other approaches evaluate the stereochemical properties of the structural model, such as its bond lengths, angles, torsion angles, planarity, and nonbond distances (e.g., the program PROCHECK) (Laskowski et al. 1993) (Table 2.2).

Finally, the position within the lipid bilayer of the protein structure obtained experimentally or computationally can also be estimated using a variety of methods, including PPM, TMDET, and iMEMBRANE (Tusnady et al. 2005; Lomize et al. 2012; Kelm et al. 2009) (Table 2.1). For example, iMEMBRANE, relies on coarse-grained MD simulations in membranous environment precalculated for proteins related to the target protein (Kelm et al. 2009).

2.2.4 Modeling Different SLC Conformations

An important step toward understanding transport by SLC transporter is the description of the conformations that the transporter undergoes during the transport cycle. Several approaches can be applied to model SLC transporters in different conformational states. First, initially shown by Forrest et al. for LeuT, the internal pseudo-symmetry of the transporter structure can be used, by swapping the symmetry-repeats (repeated halves of the transporter); essentially, one symmetry-repeat is used to model the other resulting in alternative conformation of the transporter (Forrest et al. 2008; Radestock and Forrest 2011; Faraldo-Gomez and Forrest 2011). Such approach has been applied to characterize a variety of transporters, including the glutamate transporter GltPh (Crisman et al. 2009), Na(+)/H(+) NhaA antiporter (Schushan et al. 2012), and LacY (Radestock and Forrest 2011).

Second, some transporters can be modeled based on structures of transporters that share the same fold but are only distantly related to the target (i.e., sequence identity of <10 %) (Madej et al. 2012). For example, vSGLT is currently the best template to model the human SLC5 family of Na^+ glucose co-transporter (e.g., sequence identity of 30 % with SLC5A2), but its structure was determined in only two distinct conformations (i.e., substrate bound (Faham et al. 2008) and substrate free (Watanabe et al. 2010)). However, there are total of 86 related structures of the NSS fold, representing at least six distinct conformations (Lomize et al. 2006) that can be used indirectly to model additional conformations of SLC5 members. In these cases, hybrid approaches for which low resolution data is integrated with modeling can be applied. For example, in a recent study, Madej et al. modeled an *apo*-intermediate conformation of LacY based on the atomic structure of PepT and information derived from other MFS structures including EmrD, FucP, and GlpT, in combination with low-resolution experimental data from double electron–electron resonance (DEER) measurements (Madej et al. 2012).

Third, specialized parallel computer architectures and efficient simulation algorithms have enabled researchers to perform simulations of longer times, thereby capturing important features of the transport process (Enkavi et al. 2013; Faraldo-Gomez and Forrest 2011; Khalili-Araghi et al. 2009; Lindahl and Sansom 2008). For example, employing steered molecular dynamics simulations, followed by experimental validation, Shi et al. characterized the substrate translocation pathway of LeuT, including the identification of a putative, second substrate-binding site located in the extracellular vestibule (Shi et al. 2008).

2.2.5 Molecular Docking to Comparative Models

In molecular docking, small molecules are sampled in large number of configurations and their binding modes (“poses”) are evaluated or scored based on their

Table 2.3 Molecular docking software

Method[a]	Type[b]	URL[c]	Reference[d]
DOCK	P, S	http://blaster.docking.org/	Shoichet et al. (1993), Mysinger and Shoichet (2010)
AutoDock Vina	P, S	http://vina.scripps.edu/	Trott and Olson (2010)
GOLD	P, S	http://gold.ccdc.cam.ac.uk/setup_and_run_docking.php	Verdonk et al. (2003)
RosettaLigand	P, S	https://www.rosettacommons.org/software/	Meiler and Baker (2006)

[a]*Method* marks molecular docking/virtual screening methods
[b]*Type* gives type of the prediction method; "S" and "P" correspond to web server and computer program, respectively
[c]*URL* provides the Internet address for the service
[d]*Reference* gives the primary literature describing the method

complementarity to the target protein-binding site (Shoichet 2004; Coupez and Lewis 2006; Brooijmans and Kuntz 2003; Sperandio et al. 2006). Docking algorithms are most different in their conformational space search (sampling), representation of protein–ligand interactions, and binding affinity estimation (scoring). Popular docking programs that are publically available include AutoDock Vina (Trott and Olson 2010), GOLD (Verdonk et al. 2003), RosettaLigand (Meiler and Baker 2006), and DOCK (Shoichet et al. 1993; Mysinger and Shoichet 2010) (Table 2.3). For example, DOCK generates a set of overlapping spheres in contact with the surface of the target-binding site, representing a negative image of the binding site. These spheres are then matched with ligand atoms via a graph-matching algorithm. Finally, the score of each pose is derived from a sum of van der Waals, Poisson–Boltzmann electrostatic, and ligand desolvation penalty terms (Shoichet et al. 1993; Mysinger and Shoichet 2010).

When proteins do not have experimentally determined structures, docking can also be performed against structural models calculated using comparative modeling methods (Jacobson and Sali 2004; Fan et al. 2012; Kaufmann and Meiler 2012). Although most algorithms were not optimized for docking against comparative models, Fan et al. have recently developed two distance-dependent atomic statistical potentials for scoring protein–ligand complexes that were evaluated for docking against comparative models (Fan et al. 2011). In brief, PoseScore is optimized for predicting the binding pose of a known ligand and RankScore for identifying ligands through virtual screening.

The accuracy of virtual screening against structures or models of proteins with known ligands can be estimated by the enrichment for known ligands relative to decoy compounds, calculated by docking against the tested model ("enrichment calculations") (Huang et al. 2006; Fan et al. 2009; Schlessinger et al. 2011). In particular, the enrichment curve can be obtained by plotting the percentage of actual ligands identified (y-axis) within the top ranked subset of all database compounds (x-axis on logarithmic scale) (Huang et al. 2006; Irwin and Shoichet

2005; Fan et al. 2009). The area under the curve (logAUC) of the enrichment plot for $\Delta x = 0.1$ can be calculated using Eq. (2.1):

$$\text{logAUC} = \frac{1}{\log_{10} 100/0.1} \sum_{0.1}^{100} \frac{\text{ligand}_{\text{selected}}(x)}{\text{ligand}_{\text{total}}} \Delta x \quad \text{with} \quad x = \log_{10} \frac{N_n}{N_{\text{total}}} \tag{2.1}$$

where ligand total is the number of known ligands in a database containing N_{total} compounds, and ligand selected is the number of ligands found in a given subset of N_n compounds. For example, a random selection of known ligands from a database consisting of known ligands and decoys yields a logAUC of 14.5; a selection that picks twice as many ligands at any N_{subset} as a random selection yields a logAUC of 24.5 and is considered mediocre; a selection that picks ten times as many ligands at any N_{subset} as a random selection yields a logAUC of 47.7 is considered highly accurate (Fan et al. 2012). Moreover, by selecting models based on their enrichment scores, comparative models can be optimized for protein–ligand complementarity and thus for the utility in predicting additional ligands via virtual screening (Evers et al. 2003; Cavasotto et al. 2008; Carlsson et al. 2011; Schlessinger et al. 2012). In recent years, virtual screening against comparative models has been used to identify small molecule ligands for a variety of targets, including enzymes, GPCRs, and human SLC transporters [reviewed in Jacobson and Sali (2004), Shoichet and Kobilka (2012), Schlessinger et al. (2013a) and Fan et al. (2012)].

It was proposed that the following three criteria are needed to be fulfilled for a successful virtual screening against comparative models of human SLC members (Schlessinger et al. 2013b): (1) high-quality template structure (e.g., resolution of 3 Å or lower), (2) high-sequence similarity between the target and template (e.g., sequence identity of 25 % or higher), particularly in the binding site region, and (3) the conformation of the template structure. In particular, ligand-bound conformations are likely to yield more accurate predictions because they typically represent conformational states with high affinity for ligands and because the binding site location in the model can be predicted based on its location on the template structure (de novo identification of the residues involved in ligand binding is highly nontrivial (Ghersi and Sanchez 2012)) (Fan et al. 2009; Schlessinger et al. 2013b).

2.3 Examples

2.3.1 The Norepinephrine Transporter (NET, SLC6A2)

The solute carrier 6 family (SLC6) includes 20 Na^+- and Cl^--dependent membrane transporters of neurotransmitters, amino acids, and other metabolites that are involved in a variety of biological processes (Chen et al. 2004). The SLC6 is classified into four groups based on their amino acid sequences and functions—monoamine transporters, GABA transporters, amino acid transporters, and

"orphan" transporters that include three amino acids transporters and one transporter with unknown function (Chen et al. 2004; Hahn and Blakely 2007). The norepinephrine transporter (NET, SLC6A2) is responsible for the reuptake of extracellular monoamine neurotransmitters such as norepinephrine, serotonin, and dopamine, thereby regulating adrenergic signaling pathways that are related to behavior and cardiovascular effects (Hahn and Blakely 2007; Pacholczyk et al. 1991). NET is a target for dozens of prescription (e.g., Ritalin) and recreational (cocaine) drugs that inhibit reuptake by NET to increase neurotransmitter availability for triggering adrenergic signaling.

Schlessinger et al. hypothesized that NET is involved in interacting with additional known drugs that act via polypharmacology and took modeling/docking approach to identify previously unknown NET ligand drugs (Schlessinger et al. 2011). The best template for modeling NET and other SLC6 members is LeuT which shares sequence identity of 20–25 % with the human SLC6 members as well as a conserved binding site dubbed the "S1 site." The LeuT structure has been determined in different conformations with or without ligands (Yamashita et al. 2005; Singh et al. 2007, 2008; Krishnamurthy et al. 2009). It was also shown that a putative substrate-binding site ("S2") is positioned on LeuT's surface (Shi et al. 2008; Zhao et al. 2010, 2011), and X-ray crystallography structures revealed that inhibitors can stabilize different conformations of LeuT by binding to sites overlapping with the S2 site (Claxton et al. 2010; Nyola et al. 2010). However, the S2 substrate-binding site has not been confirmed experimentally for the human SLC6 members.

Importantly, ligands transported by LeuT (amino acids) are chemically distinct from those transported by NET (positively charged monoamines), suggesting that the virtual screening against the LeuT S1-binding site is not likely to be productive for NET ligand identification and that a NET model is needed. The NET–LeuT alignment was a refined version of previously published comprehensive comparison of the SLC6 family, including eukaryotic and prokaryotic members (Beuming et al. 2006). Particularly, Beuming et al. used a variety of computational tools, including multiple sequence alignment, topology prediction, prediction of interior and lipid-exposed faces of transmembrane domains, secondary structure prediction, and even comparative modeling and previously published experimental data to construct an alignment of the SLC6 members.

NET comparative model was constructed using MODELLER and was subsequently refined by modeling key side chain using SCWRL4 (Krivov et al. 2009) and PyMOL (Fig. 2.2). For example, in the initial NET model, the side chain of Asp75, which corresponds to Gly24 in LeuT, did not face the binding site. Because an aspartate is highly conserved in the corresponding position of other SLC6 monoamine transporters, the dopamine transporter (DAT, SLC6A1) (Beuming et al. 2008) and the serotonin transporter (SERT, SLC6A4) (Kaufmann et al. 2009; Celik et al. 2008), where it makes key polar interactions with ligands (Severinsen et al. 2012; Beuming et al. 2006), Asp75 was remodeled on a fixed backbone. The utility of the model for virtual screening was estimated by the enrichment for the known ligands among the top scoring decoy compounds.

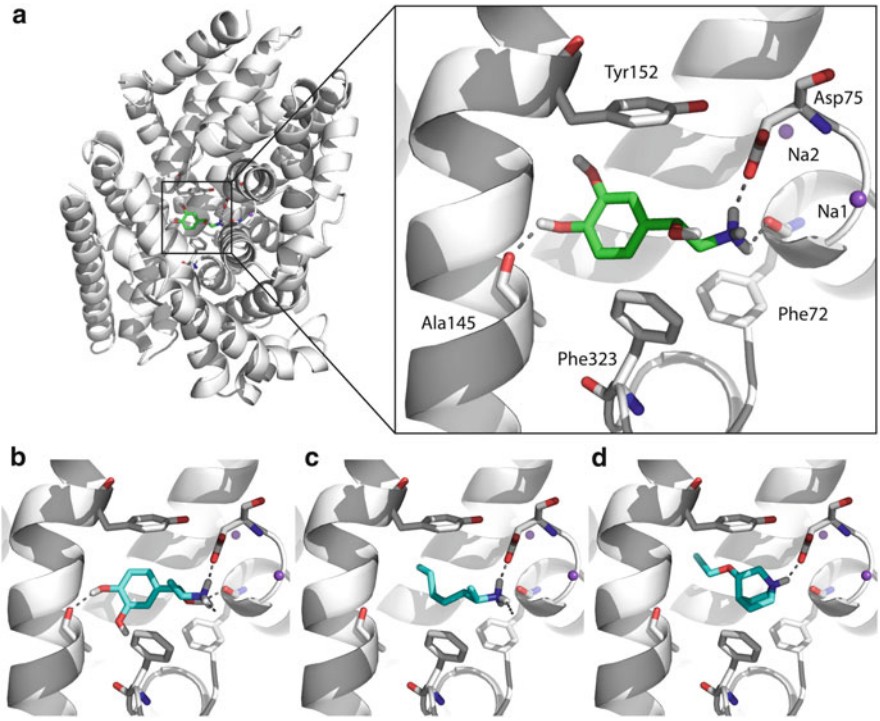

Fig. 2.2 *Predicted NET-binding site and mode of interaction with validated ligands*. (**a**) Predicted structure of the NET–norepinephrine complex. *Inset* shows the NET-binding site in complex with norepinephrine where important residues for binding are displayed as *sticks*. The known substrate norepinephrine is colored in *green*, with oxygen, nitrogen, and hydrogen atoms in *red*, *blue*, and *white*, respectively. Sodium ions are depicted as *purple* spheres. NET's transmembrane helices are shown as *white* ribbons; hydrogen bonds between norepinephrine and NET residues (e.g., Asp75) are shown as *dotted gray lines*. (**b**–**d**) Predicted binding modes of representative previously unknown prescription drugs that interact with NET (in *cyan sticks*). The drugs are (**b**) levonordefrin, and the chemically novel ligands tuaminoheptane (**c**) and talsaclidine (**d**)

The final model indicates four key binding site features that are likely to be important for NET-ligand recognition. They include (1) the polar interactions involving Asp75, (2) propensity to form interactions involving π-electrons of four aromatic residues (Phe72, Tyr152, Phe317, and Phe323), (3) hydrophobic affect involving small hydrophobic residues (e.g., Ala145 and Val148), and (4) a small binding site that limits the size of the ligands (Fig. 2.2a).

Six thousand four hundred and thirty six prescription drugs and drug-like molecules from the Kyoto Encyclopedia of Genes (KEGG DRUG) were docked against the S1-binding site of the final NET model. The top 200 predicted complexes were visually evaluated for experimental testing. In particular, molecules were selected based on the following five considerations: (1) the predicted pose was similar to predicted poses of known ligands, (2) scaffolds were predicted

repeatedly, (3) the novelty of the chemical structure of the ligand, (4) the pharmacological function of the compound, and (5) the likelihood of a false positive prediction related to the limitation of the docking program, including docking poses with high internal energies or unbound polar groups. Ten of the 18 experimentally tested molecules were identified as NET ligands, where five of these were chemically novel (Fig. 2.2b–d). Interestingly, these results reveal polypharmacology of known drugs that were not known previously to bind NET, thereby rationalizing their positive and/or negative effects. For instance, talsaclidine is a muscarinic M1 receptor ligand that failed in clinical trials for treating Alzheimer's disease, due to side effects related to adrenergic effects (e.g., high blood pressure) (Fig. 2.2d) (Adamus et al. 1995). The pharmacodynamic (Giacomini et al. 2010; Schlessinger et al. 2011) and kinetic (Schlessinger et al. 2011) properties of talsaclidine suggest that inhibition of the NET uptake might occur in clinically relevant concentrations and contribute to the positive and negative pharmacological effects of the drug.

Because of NET's role in regulating adrenergic signaling, naturally occurring mutations in NET have been associated with behavioral disorders (e.g., panic disorder) and orthostatic hypotension (Hahn and Blakely 2007). The effect of one such mutation can be rationalized based on its location on the NET structural model. Ala457Pro is strongly associated with orthostatic hypotension and tachycardia (Runkel et al. 2000), likely resulted from high levels of norepinephrine in the plasma (Paczkowski et al. 2002). Ala457 is found in TMH 9, which is located in close proximity to what corresponds to the S2-binding site. Therefore, a mutation of alanine to proline in this position might impact NET structure through (1) distortion of the α-helix geometry, (2) disruption of the helix-helix packing, and (3) decreased flexibility.

2.3.2 The GABA Transporter 2 (GAT-2, SLC6A13)

GABA is a neurotransmitter that activates the GABAergic receptors in inhibitory neurons of the mammalian central nervous system (CNS). In humans, there are four SLC6 GABA transporters (GATs) that include three CNS transporters (GAT-1, GAT-3, and BGT-1) and one peripheral transporter (GAT-2). The CNS GATs are targeted by anticonvulsants and relaxant drugs (e.g., tiagabine) that inhibit GABA reuptake, which can increase concentration of GABA available for signaling. GAT-2 (SLC6A13), however, is relatively uncharacterized transporter that is highly expressed in the liver and kidney and was suggested to be important for disposition and distribution of GABAergic drugs (Madsen et al. 2010; Nakashita et al. 1997).

GAT-2 ligand-binding mechanism and pharmacological profile were explored by structure-based discovery approach (Schlessinger et al. 2012). In particular, GAT-2 structure was modeled based on the LeuT X-ray structures in an occluded substrate-bound conformation (Yamashita et al. 2005) and in an outward-facing

inhibitor-bound conformation (Singh et al. 2008), using a refined version of the alignment developed by Beuming et al. (Beuming et al. 2006) (Fig. 2.3). Because GAT-2-binding site residues and mode of interaction with ligands have not been extensively characterized, thousands of GAT-2 configurations were sampled using sidechain modeling and energy minimization with MD simulations and were subsequently evaluated for their enrichment of known ligands among a database of known ligands and decoys. Thus, for GAT-2 modeling, enrichment scores were used for optimizing the model for protein–ligand complementarity, differently from NET modeling, where enrichment scores were used for assessing the model. Interestingly, during refinement, models in which the side chain of Glu48 faced the binding site and interacted with known ligands obtained the highest enrichment scores (and vice versa). This suggested that Glu48 plays a key role in ligand binding, which was confirmed experimentally via mutagenesis and kinetic measurements. In addition, the occluded and outward-facing GAT-2 models include minor structural rearrangements (e.g., the extracellular gate of Tyr129 and Phe288) that make additional volume accessible to solvent in the S1-binding site of the outward facing binding model, similarly to the corresponding LeuT template structures (Singh et al. 2008).

Virtual screening of 594,166 small molecule drugs, metabolites, and fragment-like molecules from the ZINC database was performed against models of the two conformations. The virtual screening results indicated that chemically distinct ligands are preferred by the different GAT-2 conformations, despite the small structural differences between their binding site conformations (Fig. 2.3). For example, larger and more hydrophobic molecules such as the muscle relaxant baclofen interact only with the outward facing model and were too large to be accommodated in the occluded conformation-binding site. Some ligands were predicted by using both models (e.g., homotaurine), thereby increasing the confidence in these predictions because the models were constructed independently.

Finally, 12 of the 31 experimentally tested molecules were identified as GAT-2 ligands, including known drugs (e.g., GABOB) and endogenous metabolites (e.g., homotaurine), where six of these ligands were chemically novel ligands of GAT-2 (e.g., baclofen). Surprisingly, the inhibitors identified from the outward-facing model, which is thought to represent an inhibited conformation, were not more potent than those predicted with the occluded model based on a substrate-bound conformation. These results indicate that the disparity between substrates and competitive inhibitors of GAT-2 is more complex than just the differences of simple physicochemical features such as size and hydrophobicity. Analogously, Albers et al. modeled the alanine–serine–cysteine transporter 2 (SLC1A5, ASCT2) based on structures of the archaeal aspartate transporter GltPh in an occluded and an outward-facing conformations (Albers et al. 2012). By using docking of serine derivatives against the two ASCT2 conformations, followed by experimental testing, they revealed that ligands identified via the screen against the occluded model were substrates, whereas ligands identified via the screen against the outward-facing inhibited conformation were inhibitors with larger and more hydrophobic side chains (Albers et al. 2012).

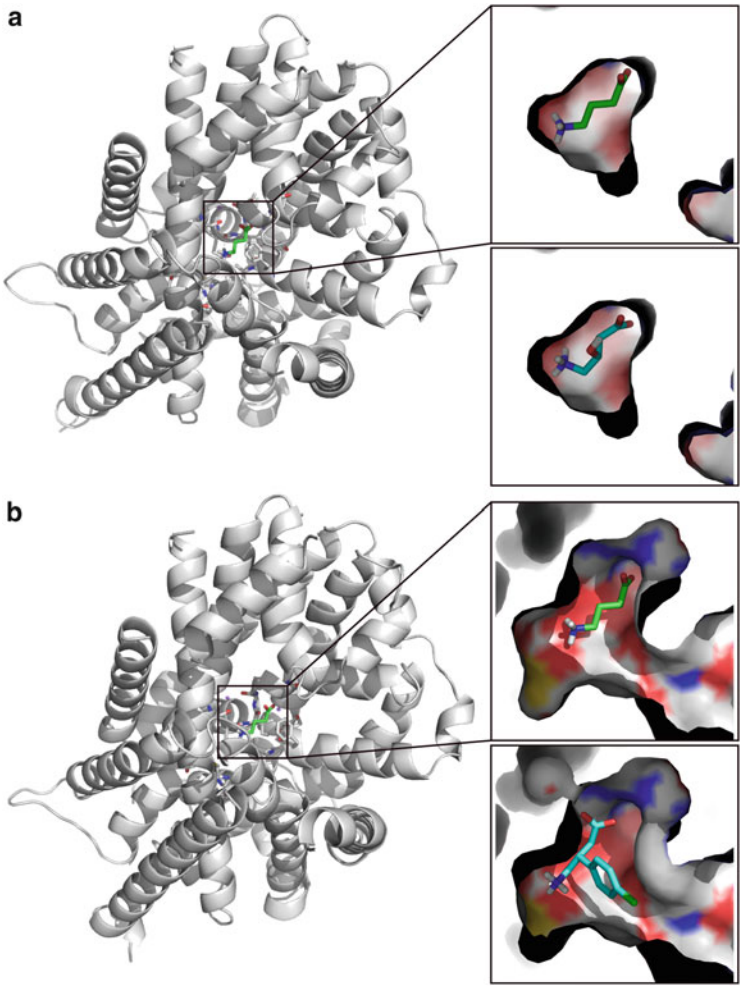

Fig. 2.3 Predicted GAT-2 structures and modes of interaction with ligands. Models of GAT-2 in occluded (**a**) and outward-facing (**b**) conformations. TMH regions are illustrated in *white ribbons*. *Inset* shows surface representation of the binding site in complex with GABA (*green*) and representative experimentally confirmed ligands that were identified from the virtual screening (*cyan*), including the GABAergic drugs vigabatrin (**a**) and baclofen (**b**). Oxygen, nitrogen, and hydrogen atoms are colored *red*, *blue*, and *white*, respectively

Comparison between models of SLC6 members and their mode of interactions with their corresponding ligands can help identifying rules for substrate specificity among members within this important family. Particularly, NET and GAT-2 share sequence identity of 45 % and their overall structures are predicted to be highly similar; however, these transporters have different substrate specificities, where NET substrates include aromatic monoamine neurotransmitters and GAT-2

substrates are typically small (7–8 heavy atoms), linear zwitterions. The following three key features likely determine the variability in substrate specificities among NET and GAT-2: (1) the number of aromatic residues (four in NET vs two in GAT-2) capable of forming hydrophobic effect and interaction involving π-electrons, (2) the number and location of amino acids with charged/polar side chains (Asp75 in NET vs Glu48 and Na1 sodium ion in GAT-2), and (3) the size and shape of the binding site where NET binding site in the occluded conformation is larger than that of GAT-2 (Schlessinger et al. 2013a).

2.3.3 LAT-1

The large neutral amino acid transporter (LAT-1) is a Na^+-independent exchanger and a member of the amino acid/polyamine/organocation transporter (APC) family. LAT-1 is expressed primarily in the blood–brain barrier (BBB) as well as in other tissues such as the placenta and testis (Kanai et al. 1998). LAT-1 is also highly upregulated in various cancerous tumors such as *glioblastoma multiforme* (GBM) (Kaira et al. 2008; Kobayashi et al. 2008), where it is thought to supply the fast-growing cancer cells with essential amino acids that are used as nutrients and signaling molecules for proliferation (Kroemer and Pouyssegur 2008; Nicklin et al. 2009). LAT-1 functions as transporter when bound to the single membrane-spanning helix glycoprotein SLC3A2 and forms the heterodimeric protein CD98, which is also a cell surface antigen associated with lymphocyte activation (Verrey et al. 2004). Therefore, LAT-1 is an important drug target for two main reasons: first, it mediates the transport of prescription drugs (e.g., gabapentin) into the CNS (Roberts et al. 2008; Alexander et al. 1994; Wang and Welty 1996), thus, potential drugs that are also LAT-1 ligands can be rationally designed for optimized BBB permeability. Second, LAT-1 can be specifically targeted for the development of cancer drugs. In brief, a drug against LAT-1 can be an inhibitor that selectively blocks its transport activity to deny the proliferating cell important nutrients or a cytotoxic substrate "hijacking" the transporter to deliver a drug against a different target in the cell (e.g., a metabolic enzyme) (Geier et al. 2013).

Sequence-based prediction methods indicate that LAT-1 includes twelve TMH (Verrey et al. 2004). Currently, there are 16 atomic structures representing four APC family members in the PDB. These structures were determined in five distinct conformations, representing different snapshots of the transport cycle (Lomize et al. 2006; Gao et al. 2009, 2010; Shaffer et al. 2009; Kowalczyk et al. 2011a; Schlessinger et al. 2010; Petrascheck et al. 2007) (Fig. 2.4a). For example, the arginine:agmatine antiporter AdiC from *E. coli* was determined in three conformations, including an "outward-facing," a "substrate-bound," and "intermediate" conformations (Gao et al. 2009, 2010; Kowalczyk et al. 2011a; Lomize et al. 2006). LAT-1 structure was recently modeled in complex with its natural substrates (Fig. 2.4) (Geier et al. 2013). Because several possible templates can be used to model LAT-1, the most optimal templates for modeling the transporter for the

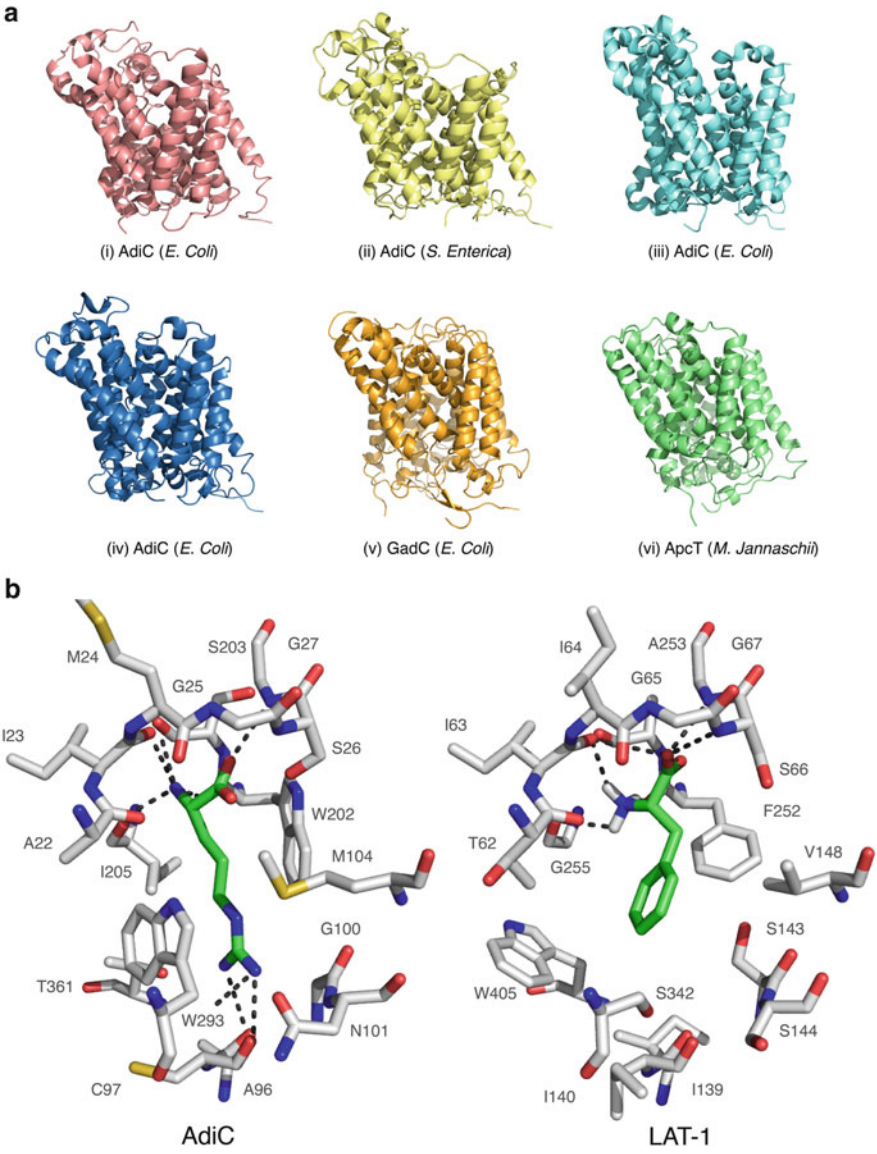

Fig. 2.4 LAT-1 modeling. (**a**) Potential template structures for modeling LAT-1. Structures belonging to the amino acid-polyamine-organocation (APC) family in OPM, including the arginine/agmatine antiporter (AdiC) in outward-facing conformation from (1) *E. coli* (PDB identifier 3lrb (Gao et al. 2009)) and (2) *Salmonella enterica* (3hqk (Fang et al. 2009)); AdiC from *E. coli* in an (3) intermediate outward-facing (3ob6 (Kowalczyk et al. 2011b)) and in a (4) substrate-bound outward-facing (3l1l (Gao et al. 2010)) conformations; (5) the glutamate/GABA antiporter (GadC) from *E. coli* in an inward conformation (4dji (Ma et al. 2012)); and (6) amino acid transporter ApcT from *M. jannaschii* in inward-facing occluded conformation (3gia (Shaffer et al. 2009)). (**b**) Binding sites of LAT-1 and AdiC. The X-ray structure of AdiC (*left panel*) and comparative

utility of virtual screening were selected by taking the following considerations: (1) sequence similarity to LAT-1, (2) structure quality, and (3) conformation, including whether the structure is ligand bound or not, and whether it is in an occluded, inward-facing, or outward-facing conformation. LAT-1 was therefore modeled based on the AdiC structure from *E. coli* in the outward-occluded arginine-bound conformation (Gao et al. 2010) and the structure of the amino acid, polyamine, and organo-cation transporter ApcT from *M. jannaschii* in an inward-*apo* conformation (Shaffer et al. 2009). The most enriching models that were ultimately subjected to virtual screening were those based on the AdiC structure from *E. coli*.

The final model of the LAT-1 in complex with its natural ligands can explain similarities and differences in ligand-binding specificity among the amino acid transporters LAT-1 and AdiC (Fig. 2.4b). In particular, backbone atoms in the binding site residues of AdiC and LAT-1 form conserved polar interactions with the carboxy and amine groups of the amino acid ligands. For example, Thr62, Ile63, and Ile64 in LAT-1 correspond to Ala22, Ile23, and Met24 in AdiC. In contrast, the binding sites of the two transporters have two key differences that likely give rise to their different ligand-binding preference (large neutral amino acids for LAT-1 vs polar amino acids for AdiC). First, LAT-1-binding site is much larger than that in AdiC, which results from substitution of amino acids with smaller side chains in LAT-1 (e.g., Val148, Gly255, and Ser342) with amino acids with larger side chains in AdiC (e.g., Met104, Ile205, and Trp293). Second, LAT-1-binding site includes more amino acids with hydrophobic and aromatic side chains than that of AdiC. For example, Thr361 in AdiC is replaced with Trp405 in LAT-1.

Virtual screening of 19,166 small molecule ligands including endogenous metabolites and prescription drugs from the KEGG database was then performed against the model binding-site. Four of the 12 high-scoring hits tested experimentally using *cis*-inhibition assays were found to inhibit uptake by LAT-1. Two of these four ligands (i.e., the anticancer agent acivicin and the tryptophan hydroxylase inhibitor fenclonine) were also characterized as substrates using a *trans*-stimulation assay (Geier et al. 2013). These results may rationalize some of the pharmacological effects of these drugs, such as the enhanced brain permeability of the CNS-active molecules acivicin and fenclonine. Finally, two of the newly discovered ligand hit inhibited proliferation of GBM cell line by distinct molecular mechanisms. In particular, acivicin is a cytotoxic substrate of LAT-1 that inhibits the activity glutamine-dependent amidotransferases in the biosynthesis of purines and pyrimidines (O'Dwyer et al. 1984); 3-iodo-L-tyrosine is a potent LAT-1 inhibitor that binds LAT-1 with stronger affinity, thereby possibly starving cancer

Fig. 2.4 (continued) model of LAT-1 (*right panel*) are shown in *light gray*. Protein atoms are shown as *sticks*; oxygen, nitrogen, and sulfur atoms are colored in *red*, *purple*, and *yellow*, respectively. Phenylalanine and arginine, substrates of LAT-1 and AdiC, respectively, are depicted as *green sticks*, and their predicted/observed hydrogen bonds with LAT-1 and AdiC, are shown as *dotted gray lines*

cells of nutrients supplied by LAT-1. These results provide useful chemical tools to characterize the role of LAT-1 in cancer metabolism as well as a starting point for optimizing the ligands for desired BBB and GBM cells permeability.

2.4 Conclusions and Future Outlook

Human SLC transporters are important for mediating transport of essential solutes, such as ions, metabolites, and prescription drugs. Recent determination of atomic structures of SLC transporters and improvement in computational structural biology methods have extended the applicability of computational structural biology to characterize many previously unmodelable human SLC transporters (see Chap. 5). We began this chapter by providing an introduction into the structures and functions of the human SLC transporters followed by the description of in silico methods that are often applied to predict the structures and substrate specificities of human SLC transporters. Finally, we illustrated how these computational methods can be applied in combination with experimental testing to characterize three important human SLC transporters.

Computational techniques are expected to continue making significant contribution to structural pharmacology investigation of membrane transporters. Particular active areas of research involve the development and application of hybrid approaches that integrate data from diverse biochemical and biophysical experiments such as NMR spectroscopy, electron microscopy, and FRET spectroscopy (e.g., Integrative Modeling Platform (Russel et al. 2012)) to model structures of unknown conformations with growing accuracy and confidence. Furthermore, the availability of increasing number of membrane protein structures will continue to enable researchers to develop more methods predicting various functional and structural aspects of membrane proteins (e.g., TMH contact prediction (Nugent and Jones 2010)). Third, new computer technologies will continue to emerge and enable researchers to perform MD simulations for longer times, which in turn will improve the state-of-the art force fields and might lead to new discoveries (Borhani and Shaw 2012).

Finally, in recent years there is a growing appreciation for the key role of the SLC transporters in human diseases such as cancer and diabetes (DeBerardinis and Thompson 2012; Wise and Thompson 2010; Vander Heiden et al. 2009; Adekola et al. 2012) and in drug ADME (Zamek-Gliszczynski et al. 2012; Giacomini et al. 2010). For example, most recently, the Food and Drug Administration (FDA) has approved canagliflozin—the first of a new class of diabetes drugs known as Na^+-glucose co-transporter 2 (SGLT2, SLC5A2) inhibitors (Traynor 2013). This understanding about the biomedical importance of the SLC transporters, coupled with the improvement in computational structural biology technology and increase in the number of SLC structures, will likely lead to additional future applications of rational structure-based drug design to membrane transporters (similarly to GPCRs). In fact, it is now feasible to target small biological

systems such as cancer metabolism pathways and whole organs (e.g., the BBB) by modeling multiple transporter targets in multiple conformations, as well as predict ligands for these targets simultaneously. In the next few years, the number of drugs rationally designed against human SLC members is, thus, expected to grow.

Acknowledgments I am grateful to Greg Madej (UCLA) and Hao Fan (UCSF) for helpful comments on the manuscript. I am also thankful to Andrej Sali, Kathleen Giacomini, Ethan Geier, Sook Wah Yee, Matthias Wittwer, Robert Stroud, Andrew Waight, Bjørn Pedersen, Arik Zur, Ligong Chen, Ursula Pieper, Ben Webb, Massimiliano Bonomi, John Irwin, and Brian Shoichet (all UCSF), as well as to Christof Grewer (SUNY Binghamton), David Smith (University of Michigan Ann Arbor), Nir Ben-Tal (TAU), Lucy Forrest (NIH), Ron Kaback (UCLA), Christine Ziegler (MPIBP Frankfurt), Reinhard Krämer (University of Cologne), and Seok-Yong Lee (Duke) for discussions about SLC transporters, structural modeling, ligand docking, and related research.

References

Abramson J, Wright EM (2009) Structure and function of Na(+)-symporters with inverted repeats. Curr Opin Struct Biol 19(4):425–432. doi:10.1016/j.sbi.2009.06.002

Adamus WS, Leonard JP, Troger W (1995) Phase I clinical trials with WAL 2014, a new muscarinic agonist for the treatment of Alzheimer's disease. Life Sci 56(11–12):883–890

Adekola K, Rosen ST, Shanmugam M (2012) Glucose transporters in cancer metabolism. Curr Opin Oncol 24(6):650–654. doi:10.1097/CCO.0b013e328356da72

Albers T, Marsiglia W, Thomas T, Gameiro A, Grewer C (2012) Defining substrate and blocker activity of alanine–serine–cysteine transporter 2 (ASCT2) ligands with novel serine analogs. Mol Pharmacol 81(3):356–365. doi:10.1124/mol.111.075648

Alexander GM, Schwartzman RJ, Grothusen JR, Gordon SW (1994) Effect of plasma levels of large neutral amino acids and degree of parkinsonism on the blood-to-brain transport of levodopa in naive and MPTP parkinsonian monkeys. Neurology 44(8):1491–1499

Altschul SF, Gish W, Miller W, Myers EW, Lipman DJ (1990) Basic local alignment search tool. J Mol Biol 215(3):403–410. doi:10.1006/jmbi.1990.9999, S0022283680799990 [pii]

Baker D, Sali A (2001) Protein structure prediction and structural genomics. Science 294 (5540):93–96

Berardi MJ, Shih WM, Harrison SC, Chou JJ (2011) Mitochondrial uncoupling protein 2 structure determined by NMR molecular fragment searching. Nature 476(7358):109–113. doi:10.1038/nature10257

Bernsel A, Viklund H, Falk J, Lindahl E, von Heijne G, Elofsson A (2008) Prediction of membrane-protein topology from first principles. Proc Natl Acad Sci U S A 105(20):7177–7181. doi:10.1073/pnas.0711151105, 0711151105 [pii]

Bernsel A, Viklund H, Hennerdal A, Elofsson A (2009) TOPCONS: consensus prediction of membrane protein topology. Nucleic Acids Res 37(Web Server issue):W465–W468. doi:10.1093/nar/gkp363

Beuming T, Kniazeff J, Bergmann ML, Shi L, Gracia L, Raniszewska K, Newman AH, Javitch JA, Weinstein H, Gether U, Loland CJ (2008) The binding sites for cocaine and dopamine in the dopamine transporter overlap. Nat Neurosci 11(7):780–789. doi:10.1038/nn.2146, nn.2146 [pii]

Beuming T, Shi L, Javitch JA, Weinstein H (2006) A comprehensive structure-based alignment of prokaryotic and eukaryotic neurotransmitter/Na^+ symporters (NSS) aids in the use of the LeuT

structure to probe NSS structure and function. Mol Pharmacol 70(5):1630–1642. doi:10.1124/mol.106.026120, mol.106.026120 [pii]

Borhani DW, Shaw DE (2012) The future of molecular dynamics simulations in drug discovery. J Comput Aided Mol Des 26(1):15–26. doi:10.1007/s10822-011-9517-y

Bowie JU, Luthy R, Eisenberg D (1991) A method to identify protein sequences that fold into a known three-dimensional structure. Science 253(5016):164–170

Brooijmans N, Kuntz ID (2003) Molecular recognition and docking algorithms. Annu Rev Biophys Biomol Struct 32:335–373. doi:10.1146/annurev.biophys.32.110601.142532

Carlsson J, Coleman RG, Setola V, Irwin JJ, Fan H, Schlessinger A, Sali A, Roth BL, Shoichet BK (2011) Ligand discovery from a dopamine D3 receptor homology model and crystal structure. Nat Chem Biol 7(11):769–778. doi:10.1038/nchembio.662

Cavasotto CN, Orry AJ, Murgolo NJ, Czarniecki MF, Kocsi SA, Hawes BE, O'Neill KA, Hine H, Burton MS, Voigt JH, Abagyan RA, Bayne ML, Monsma FJ Jr (2008) Discovery of novel chemotypes to a G-protein-coupled receptor through ligand-steered homology modeling and structure-based virtual screening. J Med Chem 51(3):581–588. doi:10.1021/jm070759m

Celik L, Sinning S, Severinsen K, Hansen CG, Moller MS, Bols M, Wiborg O, Schiott B (2008) Binding of serotonin to the human serotonin transporter. Molecular modeling and experimental validation. J Am Chem Soc 130(12):3853–3865. doi:10.1021/ja076403h

Chang JM, Di Tommaso P, Taly JF, Notredame C (2012) Accurate multiple sequence alignment of transmembrane proteins with PSI-Coffee. BMC Bioinformatics 13(Suppl 4):S1. doi:10.1186/1471-2105-13-S4-S1

Chen NH, Reith ME, Quick MW (2004) Synaptic uptake and beyond: the sodium- and chloride-dependent neurotransmitter transporter family SLC6. Pflugers Arch 447(5):519–531. doi:10.1007/s00424-003-1064-5

Choi JH, Yee SW, Ramirez AH, Morrissey KM, Jang GH, Joski PJ, Mefford JA, Hesselson SE, Schlessinger A, Jenkins G, Castro RA, Johns SJ, Stryke D, Sali A, Ferrin TE, Witte JS, Kwok PY, Roden DM, Wilke RA, McCarty CA, Davis RL, Giacomini KM (2011) A common 5'-UTR variant in MATE2-K is associated with poor response to metformin. Clin Pharmacol Ther 90(5):674–684. doi:10.1038/clpt.2011.165

Claxton DP, Quick M, Shi L, de Carvalho FD, Weinstein H, Javitch JA, McHaourab HS (2010) Ion/substrate-dependent conformational dynamics of a bacterial homolog of neurotransmitter: sodium symporters. Nat Struct Mol Biol 17(7):822–829. doi:10.1038/nsmb.1854

Coupez B, Lewis RA (2006) Docking and scoring—theoretically easy, practically impossible? Curr Med Chem 13(25):2995–3003

Crisman TJ, Qu S, Kanner BI, Forrest LR (2009) Inward-facing conformation of glutamate transporters as revealed by their inverted-topology structural repeats. Proc Natl Acad Sci U S A 106(49):20752–20757. doi:10.1073/pnas.0908570106

DeBerardinis RJ, Thompson CB (2012) Cellular metabolism and disease: what do metabolic outliers teach us? Cell 148(6):1132–1144. doi:10.1016/j.cell.2012.02.032

Dresser MJ, Gray AT, Giacomini KM (2000) Kinetic and selectivity differences between rodent, rabbit, and human organic cation transporters (OCT1). J Pharmacol Exp Ther 292(3):1146–1152

Elofsson A, von Heijne G (2007) Membrane protein structure: prediction versus reality. Annu Rev Biochem 76:125–140. doi:10.1146/annurev.biochem.76.052705.163539

Enkavi G, Li J, Mahinthichaichan P, Wen PC, Huang Z, Shaikh SA, Tajkhorshid E (2013) Simulation studies of the mechanism of membrane transporters. Methods Mol Biol 924:361–405. doi:10.1007/978-1-62703-017-5_14

Eramian D, Eswar N, Shen MY, Sali A (2008) How well can the accuracy of comparative protein structure models be predicted? Protein Sci 17(11):1881–1893. doi:10.1110/ps.036061.108, ps.036061.108 [pii]

Evers A, Gohlke H, Klebe G (2003) Ligand-supported homology modelling of protein binding-sites using knowledge-based potentials. J Mol Biol 334(2):327–345

Eyre TA, Partridge L, Thornton JM (2004) Computational analysis of alpha-helical membrane protein structure: implications for the prediction of 3D structural models. Protein Eng Des Sel 17(8):613–624. doi:10.1093/protein/gzh072

Faham S, Watanabe A, Besserer GM, Cascio D, Specht A, Hirayama BA, Wright EM, Abramson J (2008) The crystal structure of a sodium galactose transporter reveals mechanistic insights into Na^+/sugar symport. Science 321(5890):810–814

Fan H, Irwin JJ, Sali A (2012) Virtual ligand screening against comparative protein structure models. Methods Mol Biol 819:105–126. doi:10.1007/978-1-61779-465-0_8

Fan H, Irwin JJ, Webb BM, Klebe G, Shoichet BK, Sali A (2009) Molecular docking screens using comparative models of proteins. J Chem Inf Model 49(11):2512–2527. doi:10.1021/ci9003706

Fan H, Schneidman-Duhovny D, Irwin JJ, Dong G, Shoichet BK, Sali A (2011) Statistical potential for modeling and ranking of protein–ligand interactions. J Chem Inf Model 51 (12):3078–3092. doi:10.1021/ci200377u

Fang Y, Jayaram H, Shane T, Kolmakova-Partensky L, Wu F, Williams C, Xiong Y, Miller C (2009) Structure of a prokaryotic virtual proton pump at 3.2 A resolution. Nature 460 (7258):1040–1043. doi:10.1038/nature08201, nature08201 [pii]

Faraldo-Gomez JD, Forrest LR (2011) Modeling and simulation of ion-coupled and ATP-driven membrane proteins. Curr Opin Struct Biol 21(2):173–179. doi:10.1016/j.sbi.2011.01.013

Feng B, Dresser MJ, Shu Y, Johns SJ, Giacomini KM (2001) Arginine 454 and lysine 370 are essential for the anion specificity of the organic anion transporter, rOAT3. Biochemistry 40 (18):5511–5520, bi002841o [pii]

Fernandez-Fuentes N, Zhai J, Fiser A (2006) ArchPRED: a template based loop structure prediction server. Nucleic Acids Res 34(Web Server issue):W173–W176. doi:10.1093/nar/gkl113

Fiser A, Sali A (2003) ModLoop: automated modeling of loops in protein structures. Bioinformatics 19(18):2500–2501

Forrest LR (2013) Structural biology. (Pseudo-)symmetrical transport. Science 339(6118):399–401. doi:10.1126/science.1228465

Forrest LR, Kramer R, Ziegler C (2011) The structural basis of secondary active transport mechanisms. Biochim Biophys Acta 1807(2):167–188. doi:10.1016/j.bbabio.2010.10.014

Forrest LR, Rudnick G (2009) The rocking bundle: a mechanism for ion-coupled solute flux by symmetrical transporters. Physiology (Bethesda) 24:377–386. doi:10.1152/physiol.00030.2009, 24/6/377 [pii]

Forrest LR, Tang CL, Honig B (2006) On the accuracy of homology modeling and sequence alignment methods applied to membrane proteins. Biophys J 91(2):508–517

Forrest LR, Zhang YW, Jacobs MT, Gesmonde J, Xie L, Honig BH, Rudnick G (2008) Mechanism for alternating access in neurotransmitter transporters. Proc Natl Acad Sci U S A 105 (30):10338–10343

Gao X, Lu F, Zhou L, Dang S, Sun L, Li X, Wang J, Shi Y (2009) Structure and mechanism of an amino acid antiporter. Science 324(5934):1565–1568. doi:10.1126/science.1173654, 1173654 [pii]

Gao X, Zhou L, Jiao X, Lu F, Yan C, Zeng X, Wang J, Shi Y (2010) Mechanism of substrate recognition and transport by an amino acid antiporter. Nature 463(7282):828–832. doi:10.1038/nature08741

Geier EG, Schlessinger A, Fan H, Gable JE, Irwin JJ, Sali A, Giacomini KM (2013) Structure-based ligand discovery for the large-neutral amino acid transporter 1, LAT-1. Proc Natl Acad Sci U S A 110(14):5480–5485. doi:10.1073/pnas.1218165110

Gether U, Andersen PH, Larsson OM, Schousboe A (2006) Neurotransmitter transporters: molecular function of important drug targets. Trends Pharmacol Sci 27(7):375–383

Ghersi D, Sanchez R (2012) Automated identification of binding sites for phosphorylated ligands in protein structures. Proteins 80(10):2347–2358. doi:10.1002/prot.24117

Giacomini KM, Huang SM, Tweedie DJ, Benet LZ, Brouwer KL, Chu X, Dahlin A, Evers R, Fischer V, Hillgren KM, Hoffmaster KA, Ishikawa T, Keppler D, Kim RB, Lee CA, Niemi M, Polli JW, Sugiyama Y, Swaan PW, Ware JA, Wright SH, Yee SW, Zamek-Gliszczynski MJ,

Zhang L (2010) Membrane transporters in drug development. Nat Rev Drug Discov 9(3):215–236. doi:10.1038/nrd3028

Gruswitz F, Chaudhary S, Ho JD, Schlessinger A, Pezeshki B, Ho CM, Sali A, Westhoff CM, Stroud RM (2010) Function of human Rh based on structure of RhCG at 2.1 A. Proc Natl Acad Sci U S A 107(21):9638–9643. doi:10.1073/pnas.1003587107

Guan L, Kaback HR (2006) Lessons from lactose permease. Annu Rev Biophys Biomol Struct 35:67–91. doi:10.1146/annurev.biophys.35.040405.102005

Guastella J, Nelson N, Nelson H, Czyzyk L, Keynan S, Miedel MC, Davidson N, Lester HA, Kanner BI (1990) Cloning and expression of a rat brain GABA transporter. Science 249 (4974):1303–1306

Hahn MK, Blakely RD (2007) The functional impact of SLC6 transporter genetic variation. Annu Rev Pharmacol Toxicol 47:401–441. doi:10.1146/annurev.pharmtox.47.120505.105242

Harrington SE, Ben-Tal N (2009) Structural determinants of transmembrane helical proteins. Structure 17(8):1092–1103. doi:10.1016/j.str.2009.06.009

Hediger MA, Romero MF, Peng JB, Rolfs A, Takanaga H, Bruford EA (2004) The ABCs of solute carriers: physiological, pathological and therapeutic implications of human membrane transport proteinsIntroduction. Pflugers Arch 447(5):465–468

Hess B, Kutzner C, van der Spoel D, Lindahl E (2008) GROMACS 4: algorithms for highly efficient, load-balanced, and scalable molecular simulation. J Chem Theory Comput 4(3):435–447. doi:10.1021/ct700301q

Hill JR, Deane CM (2013) MP-T: improving membrane protein alignment for structure prediction. Bioinformatics 29(1):54–61. doi:10.1093/bioinformatics/bts640

Hopf TA, Colwell LJ, Sheridan R, Rost B, Sander C, Marks DS (2012) Three-dimensional structures of membrane proteins from genomic sequencing. Cell 149(7):1607–1621. doi:10.1016/j.cell.2012.04.012

Huang N, Shoichet BK, Irwin JJ (2006) Benchmarking sets for molecular docking. J Med Chem 49 (23):6789–6801. doi:10.1021/jm0608356

Irwin JJ, Shoichet BK (2005) ZINC—a free database of commercially available compounds for virtual screening. J Chem Inf Model 45(1):177–182

Jacobson M, Sali A (2004) Comparative protein structure modeling and its applications to drug discovery. In: Overington J (ed) Annual reports in medicinal chemistry, vol 39. Inpharmatica Ltd, London, pp 259–276

Jacobson MP, Pincus DL, Rapp CS, Day TJ, Honig B, Shaw DE, Friesner RA (2004) A hierarchical approach to all-atom protein loop prediction. Proteins 55(2):351–367. doi:10.1002/prot.10613

Jardetzky O (1966) Simple allosteric model for membrane pumps. Nature 211(5052):969–970

Johnson ZL, Cheong CG, Lee SY (2012) Crystal structure of a concentrative nucleoside transporter from *Vibrio cholerae* at 2.4 A. Nature 483(7390):489–493. doi:10.1038/nature10882

Kaira K, Oriuchi N, Imai H, Shimizu K, Yanagitani N, Sunaga N, Hisada T, Tanaka S, Ishizuka T, Kanai Y, Endou H, Nakajima T, Mori M (2008) Prognostic significance of L-type amino acid transporter 1 expression in resectable stage I–III nonsmall cell lung cancer. Br J Cancer 98 (4):742–748. doi:10.1038/sj.bjc.6604235

Kall L, Krogh A, Sonnhammer EL (2005) An HMM posterior decoder for sequence feature prediction that includes homology information. Bioinformatics 21(Suppl 1):i251–i257. doi:10.1093/bioinformatics/bti1014

Kanai Y, Segawa H, Miyamoto K, Uchino H, Takeda E, Endou H (1998) Expression cloning and characterization of a transporter for large neutral amino acids activated by the heavy chain of 4 F2 antigen (CD98). J Biol Chem 273(37):23629–23632

Kanner BI, Zomot E (2008) Sodium-coupled neurotransmitter transporters. Chem Rev 108 (5):1654–1668. doi:10.1021/cr078246a

Katoh K, Toh H (2008) Recent developments in the MAFFT multiple sequence alignment program. Brief Bioinform 9(4):286–298. doi:10.1093/bib/bbn013

Kaufmann KW, Dawson ES, Henry LK, Field JR, Blakely RD, Meiler J (2009) Structural determinants of species-selective substrate recognition in human and Drosophila serotonin transporters revealed through computational docking studies. Proteins 74(3):630–642. doi:10.1002/prot.22178

Kaufmann KW, Meiler J (2012) Using RosettaLigand for small molecule docking into comparative models. PLoS One 7(12):e50769. doi:10.1371/journal.pone.0050769

Kelm S, Shi J, Deane CM (2009) iMembrane: homology-based membrane-insertion of proteins. Bioinformatics 25(8):1086–1088. doi:10.1093/bioinformatics/btp102

Kelm S, Shi J, Deane CM (2010) MEDELLER: homology-based coordinate generation for membrane proteins. Bioinformatics 26(22):2833–2840. doi:10.1093/bioinformatics/btq554

Kernytsky A, Rost B (2003) Static benchmarking of membrane helix predictions. Nucleic Acids Res 31(13):3642–3644

Khafizov K, Staritzbichler R, Stamm M, Forrest LR (2010) A study of the evolution of inverted-topology repeats from LeuT-fold transporters using AlignMe. Biochemistry 49(50):10702–10713. doi:10.1021/bi101256x

Khalili-Araghi F, Gumbart J, Wen PC, Sotomayor M, Tajkhorshid E, Schulten K (2009) Molecular dynamics simulations of membrane channels and transporters. Curr Opin Struct Biol 19(2):128–137. doi:10.1016/j.sbi.2009.02.011

Kiefer F, Arnold K, Kunzli M, Bordoli L, Schwede T (2009) The SWISS-MODEL repository and associated resources. Nucleic Acids Res 37(Database issue):D387–D392. doi:10.1093/nar/gkn750

Kobayashi K, Ohnishi A, Promsuk J, Shimizu S, Kanai Y, Shiokawa Y, Nagane M (2008) Enhanced tumor growth elicited by L-type amino acid transporter 1 in human malignant glioma cells. Neurosurgery 62(2):493–503. doi:10.1227/01.neu.0000316018.51292.19, discussion 503–494

Kowalczyk L, Ratera M, Paladino A, Bartoccioni P, Errasti-Murugarren E, Valencia E, Portella G, Bial S, Zorzano A, Fita I, Orozco M, Carpena X, Vazquez-Ibar JL, Palacin M (2011a) Molecular basis of substrate-induced permeation by an amino acid antiporter. Proc Natl Acad Sci U S A 108(10):3935–3940. doi:10.1073/pnas.1018081108

Kowalczyk L, Ratera M, Paladino A, Bartoccioni P, Errasti-Murugarren E, Valencia E, Portella G, Bial S, Zorzano A, Fita I, Orozco M, Carpena X, Vazquez-Ibar JL, Palacin M (2011b) Molecular basis of substrate-induced permeation by an amino acid antiporter. Proc Natl Acad Sci U S A 108(10):3935–3940. doi:10.1073/pnas.1018081108

Krishnamurthy H, Gouaux E (2012) X-ray structures of LeuT in substrate-free outward-open and apo inward-open states. Nature 481(7382):469–474. doi:10.1038/nature10737

Krishnamurthy H, Piscitelli CL, Gouaux E (2009) Unlocking the molecular secrets of sodium-coupled transporters. Nature 459(7245):347–355. doi:10.1038/nature08143, nature08143 [pii]

Krivov GG, Shapovalov MV, Dunbrack RL Jr (2009) Improved prediction of protein side-chain conformations with SCWRL4. Proteins 77(4):778–795. doi:10.1002/prot.22488

Kroemer G, Pouyssegur J (2008) Tumor cell metabolism: cancer's Achilles' heel. Cancer Cell 13(6):472–482. doi:10.1016/j.ccr.2008.05.005

Kyte J, Doolittle RF (1982) A simple method for displaying the hydropathic character of a protein. J Mol Biol 157(1):105–132

Laskowski RA, Moss DS, Thornton JM (1993) Main-chain bond lengths and bond angles in protein structures. J Mol Biol 231(4):1049–1067. doi:10.1006/jmbi.1993.1351

Lindahl E, Sansom MS (2008) Membrane proteins: molecular dynamics simulations. Curr Opin Struct Biol 18(4):425–431. doi:10.1016/j.sbi.2008.02.003

Lindorff-Larsen K, Piana S, Palmo K, Maragakis P, Klepeis JL, Dror RO, Shaw DE (2010) Improved side-chain torsion potentials for the Amber ff99SB protein force field. Proteins 78(8):1950–1958. doi:10.1002/prot.22711

Lomize MA, Lomize AL, Pogozheva ID, Mosberg HI (2006) OPM: orientations of proteins in membranes database. Bioinformatics 22(5):623–625. doi:10.1093/bioinformatics/btk023, btk023 [pii]

Lomize MA, Pogozheva ID, Joo H, Mosberg HI, Lomize AL (2012) OPM database and PPM web server: resources for positioning of proteins in membranes. Nucleic Acids Res 40(Database issue):D370–D376. doi:10.1093/nar/gkr703

Lorber DM, Shoichet BK (1998) Flexible ligand docking using conformational ensembles. Protein Sci 7(4):938–950. doi:10.1002/pro.5560070411

Lu F, Li S, Jiang Y, Jiang J, Fan H, Lu G, Deng D, Dang S, Zhang X, Wang J, Yan N (2011) Structure and mechanism of the uracil transporter UraA. Nature 472(7342):243–246. doi:10.1038/nature09885

Ma D, Lu P, Yan C, Fan C, Yin P, Wang J, Shi Y (2012) Structure and mechanism of a glutamate–GABA antiporter. Nature 483(7391):632–636. doi:10.1038/nature10917

Madej MG, Dang S, Yan N, Kaback HR (2013) Evolutionary mix-and-match with MFS transporters. Proc Natl Acad Sci U S A 110(15):5870–5874. doi:10.1073/pnas.1303538110

Madej MG, Soro SN, Kaback HR (2012) Apo-intermediate in the transport cycle of lactose permease (LacY). Proc Natl Acad Sci U S A 109(44):E2970–E2978. doi:10.1073/pnas.1211183109

Madhusudhan MS, Webb BM, Marti-Renom MA, Eswar N, Sali A (2009) Alignment of multiple protein structures based on sequence and structure features. Protein Eng Des Sel 22(9):569–574. doi:10.1093/protein/gzp040, gzp040 [pii]

Madsen KK, White HS, Schousboe A (2010) Neuronal and non-neuronal GABA transporters as targets for antiepileptic drugs. Pharmacol Ther 125(3):394–401. doi:10.1016/j.pharmthera.2009.11.007

Marks DS, Colwell LJ, Sheridan R, Hopf TA, Pagnani A, Zecchina R, Sander C (2011) Protein 3D structure computed from evolutionary sequence variation. PLoS One 6(12):e28766. doi:10.1371/journal.pone.0028766

Marti-Renom MA, Stuart AC, Fiser A, Sanchez R, Melo F, Sali A (2000) Comparative protein structure modeling of genes and genomes. Annu Rev Biophys Biomol Struct 29:291–325. doi:10.1146/annurev.biophys.29.1.291

Meiler J, Baker D (2006) ROSETTALIGAND: protein-small molecule docking with full side-chain flexibility. Proteins 65(3):538–548. doi:10.1002/prot.21086

Melo F, Sanchez R, Sali A (2002) Statistical potentials for fold assessment. Protein Sci 11(2):430–448

Murzin AG, Brenner SE, Hubbard T, Chothia C (1995) SCOP: a structural classification of proteins database for the investigation of sequences and structures. J Mol Biol 247(4):536–540. doi:10.1006/jmbi.1995.0159, S0022283685701593 [pii]

Mysinger MM, Shoichet BK (2010) Rapid context-dependent ligand desolvation in molecular docking. J Chem Inf Model 50(9):1561–1573. doi:10.1021/ci100214a

Nakashita M, Sasaki K, Sakai N, Saito N (1997) Effects of tricyclic and tetracyclic antidepressants on the three subtypes of GABA transporter. Neurosci Res 29(1):87–91

Newstead S, Drew D, Cameron AD, Postis VL, Xia X, Fowler PW, Ingram JC, Carpenter EP, Sansom MS, McPherson MJ, Baldwin SA, Iwata S (2011) Crystal structure of a prokaryotic homologue of the mammalian oligopeptide–proton symporters, PepT1 and PepT2. EMBO J 30(2):417–426. doi:10.1038/emboj.2010.309

Nicklin P, Bergman P, Zhang B, Triantafellow E, Wang H, Nyfeler B, Yang H, Hild M, Kung C, Wilson C, Myer VE, MacKeigan JP, Porter JA, Wang YK, Cantley LC, Finan PM, Murphy LO (2009) Bidirectional transport of amino acids regulates mTOR and autophagy. Cell 136(3):521–534. doi:10.1016/j.cell.2008.11.044

Nugent T, Jones DT (2009) Transmembrane protein topology prediction using support vector machines. BMC Bioinforma 10:159. doi:10.1186/1471-2105-10-159

Nugent T, Jones DT (2010) Predicting transmembrane helix packing arrangements using residue contacts and a force-directed algorithm. PLoS Comput Biol 6(3):e1000714. doi:10.1371/journal.pcbi.1000714

Nugent T, Jones DT (2012) Membrane protein structural bioinformatics. J Struct Biol 179(3):327–337. doi:10.1016/j.jsb.2011.10.008

Nyola A, Karpowich NK, Zhen J, Marden J, Reith ME, Wang DN (2010) Substrate and drug binding sites in LeuT. Curr Opin Struct Biol 20(4):415–422. doi:10.1016/j.sbi.2010.05.007

O'Dwyer PJ, Alonso MT, Leyland-Jones B (1984) Acivicin: a new glutamine antagonist in clinical trials. J Clin Oncol 2(9):1064–1071

Pacholczyk T, Blakely RD, Amara SG (1991) Expression cloning of a cocaine- and antidepressant-sensitive human noradrenaline transporter. Nature 350(6316):350–354. doi:10.1038/350350a0

Paczkowski FA, Bonisch H, Bryan-Lluka LJ (2002) Pharmacological properties of the naturally occurring Ala(457)Pro variant of the human norepinephrine transporter. Pharmacogenetics 12 (2):165–173

Pedersen BP, Kumar H, Waight AB, Risenmay AJ, Roe-Zurz Z, Chau BH, Schlessinger A, Bonomi M, Harries W, Sali A, Johri AK, Stroud RM (2013) Crystal structure of a eukaryotic phosphate transporter. Nature. doi:10.1038/nature12042

Pei J, Kim BH, Grishin NV (2008) PROMALS3D: a tool for multiple protein sequence and structure alignments. Nucleic Acids Res 36(7):2295–2300. doi:10.1093/nar/gkn072

Perez C, Ziegler C (2013) Mechanistic aspects of sodium-binding sites in LeuT-like fold symporters. Biol Chem. doi:10.1515/hsz-2012-0336

Petrascheck M, Ye X, Buck LB (2007) An antidepressant that extends lifespan in adult Caenorhabditis elegans. Nature 450(7169):553–556. doi:10.1038/nature05991, nature05991 [pii]

Pettersen EF, Goddard TD, Huang CC, Couch GS, Greenblatt DM, Meng EC, Ferrin TE (2004) UCSF Chimera—a visualization system for exploratory research and analysis. J Comput Chem 25(13):1605–1612. doi:10.1002/jcc.20084

Pieper U, Schlessinger A, Kloppmann E, Chang GA, Chou JJ, Dumont ME, Fox BG, Fromme P, Hendrickson WA, Malkowski MG, Rees DC, Stokes DL, Stowell MH, Wiener MC, Rost B, Stroud RM, Stevens RC, Sali A (2013) Coordinating the impact of structural genomics on the human alpha-helical transmembrane proteome. Nat Struct Mol Biol 20(2):135–138. doi:10.1038/nsmb.2508

Pieper U, Webb BM, Barkan DT, Schneidman-Duhovny D, Schlessinger A, Braberg H, Yang Z, Meng EC, Pettersen EF, Huang CC, Datta RS, Sampathkumar P, Madhusudhan MS, Sjolander K, Ferrin TE, Burley SK, Sali A (2011) ModBase, a database of annotated comparative protein structure models, and associated resources. Nucleic Acids Res 39(Database issue):D465–D474. doi:10.1093/nar/gkq1091

Pirovano W, Feenstra KA, Heringa J (2008) PRALINETM: a strategy for improved multiple alignment of transmembrane proteins. Bioinformatics 24(4):492–497. doi:10.1093/bioinformatics/btm636

Povey S, Lovering R, Bruford E, Wright M, Lush M, Wain H (2001) The HUGO gene nomenclature committee (HGNC). Hum Genet 109(6):678–680. doi:10.1007/s00439-001-0615-0

Punta M, Forrest LR, Bigelow H, Kernytsky A, Liu J, Rost B (2007) Membrane protein prediction methods. Methods 41(4):460–474. doi:10.1016/j.ymeth.2006.07.026

Radestock S, Forrest LR (2011) The alternating-access mechanism of MFS transporters arises from inverted-topology repeats. J Mol Biol 407(5):698–715. doi:10.1016/j.jmb.2011.02.008

Ressl S, Terwisscha van Scheltinga AC, Vonrhein C, Ott V, Ziegler C (2009) Molecular basis of transport and regulation in the Na(+)/betaine symporter BetP. Nature 458(7234):47–52. doi:10.1038/nature07819, nature07819 [pii]

Roberts LM, Black DS, Raman C, Woodford K, Zhou M, Haggerty JE, Yan AT, Cwirla SE, Grindstaff KK (2008) Subcellular localization of transporters along the rat blood–brain barrier and blood–cerebral-spinal fluid barrier by in vivo biotinylation. Neuroscience 155(2):423–438. doi:10.1016/j.neuroscience.2008.06.015

Rohl CA, Strauss CE, Misura KM, Baker D (2004) Protein structure prediction using Rosetta. Methods Enzymol 383:66–93. doi:10.1016/S0076-6879(04)83004-0

Rost B, Casadio R, Fariselli P, Sander C (1995) Transmembrane helices predicted at 95 % accuracy. Protein Sci 4(3):521–533

Rost B, Liu J, Nair R, Wrzeszczynski KO, Ofran Y (2003) Automatic prediction of protein function. Cell Mol Life Sci 60(12):2637–2650. doi:10.1007/s00018-003-3114-8

Runkel F, Bruss M, Nothen MM, Stober G, Propping P, Bonisch H (2000) Pharmacological properties of naturally occurring variants of the human norepinephrine transporter. Pharmacogenetics 10(5):397–405

Russel D, Lasker K, Webb B, Velazquez-Muriel J, Tjioe E, Schneidman-Duhovny D, Peterson B, Sali A (2012) Putting the pieces together: integrative modeling platform software for structure determination of macromolecular assemblies. PLoS Biol 10(1):e1001244. doi:10.1371/journal.pbio.1001244

Saier MH Jr (2000) A functional-phylogenetic classification system for transmembrane solute transporters. Microbiol Mol Biol Rev 64(2):354–411

Saier MH Jr, Yen MR, Noto K, Tamang DG, Elkan C (2009) The transporter classification database: recent advances. Nucleic Acids Res 37(Database issue):D274–D278. doi:10.1093/nar/gkn862, doi:gkn862 [pii]

Sali A, Blundell TL (1993) Comparative protein modelling by satisfaction of spatial restraints. J Mol Biol 234(3):779–815

Sanchez R, Sali A (1998) Large-scale protein structure modeling of the *Saccharomyces cerevisiae* genome. Proc Natl Acad Sci U S A 95(23):13597–13602

Schlessinger A, Geier E, Fan H, Irwin JJ, Shoichet BK, Giacomini KM, Sali A (2011) Structure-based discovery of prescription drugs that interact with the norepinephrine transporter, NET. Proc Natl Acad Sci U S A 108(38):15810–15815. doi:10.1073/pnas.1106030108

Schlessinger A, Khuri N, Giacomini KM, Sali A (2013a) Molecular modeling and ligand docking for solute carrier (SLC) transporters. Curr Top Med Chem 13(7):843–856

Schlessinger A, Matsson P, Shima JE, Pieper U, Yee SW, Kelly L, Apeltsin L, Stroud RM, Ferrin TE, Giacomini KM, Sali A (2010) Comparison of human solute carriers. Protein Sci 19 (3):412–428. doi:10.1002/pro.320

Schlessinger A, Wittwer MB, Dahlin A, Khuri N, Bonomi M, Fan H, Giacomini KM, Sali A (2012) High selectivity of the gamma-aminobutyric acid transporter 2 (GAT-2, SLC6A13) revealed by structure-based approach. J Biol Chem 287(45):37745–37756. doi:10.1074/jbc.M112.388157

Schlessinger A, Yee SW, Sali A, Giacomini KM (2013) SLC classification: an update. Clin Pharmacol Ther 94(1):19–23. doi:10.1038/clpt.2013.73

Schulze S, Koster S, Geldmacher U, Terwisscha van Scheltinga AC, Kuhlbrandt W (2010) Structural basis of Na(+)-independent and cooperative substrate/product antiport in CaiT. Nature 467(7312):233–236. doi:10.1038/nature09310

Schushan M, Rimon A, Haliloglu T, Forrest LR, Padan E, Ben-Tal N (2012) A model-structure of a periplasm-facing state of the NhaA antiporter suggests the molecular underpinnings of pH-induced conformational changes. J Biol Chem 287(22):18249–18261. doi:10.1074/jbc.M111.336446

Severinsen K, Kraft JF, Koldso H, Vinberg KA, Rothman RB, Partilla JS, Wiborg O, Blough B, Schiott B, Sinning S (2012) Binding of the amphetamine-like 1-phenyl-piperazine to monoamine transporters. ACS Chem Neurosci 3(9):693–705. doi:10.1021/cn300040f

Shaffer PL, Goehring A, Shankaranarayanan A, Gouaux E (2009) Structure and mechanism of a Na^+-independent amino acid transporter. Science 325(5943):1010–1014. doi:10.1126/science.1176088, 1176088 [pii]

Shaw DE, Maragakis P, Lindorff-Larsen K, Piana S, Dror RO, Eastwood MP, Bank JA, Jumper JM, Salmon JK, Shan Y, Wriggers W (2010) Atomic-level characterization of the structural dynamics of proteins. Science 330(6002):341–346. doi:10.1126/science.1187409

Shen MY, Sali A (2006) Statistical potential for assessment and prediction of protein structures. Protein Sci 15(11):2507–2524

Shi L, Quick M, Zhao Y, Weinstein H, Javitch JA (2008) The mechanism of a neurotransmitter: sodium symporter—inward release of Na^+ and substrate is triggered by substrate in a second

binding site. Mol Cell 30(6):667–677. doi:10.1016/j.molcel.2008.05.008, S1097-2765(08)00359-6 [pii]
Shi L, Weinstein H (2010) Conformational rearrangements to the intracellular open states of the LeuT and ApcT transporters are modulated by common mechanisms. Biophys J 99(12):L103–L105. doi:10.1016/j.bpj.2010.10.003
Shoichet BK (2004) Virtual screening of chemical libraries. Nature 432(7019):862–865
Shoichet BK, Kobilka BK (2012) Structure-based drug screening for G-protein-coupled receptors. Trends Pharmacol Sci 33(5):268–272. doi:10.1016/j.tips.2012.03.007
Shoichet BK, Stroud RM, Santi DV, Kuntz ID, Perry KM (1993) Structure-based discovery of inhibitors of thymidylate synthase. Science 259(5100):1445–1450
Shu Y, Brown C, Castro RA, Shi RJ, Lin ET, Owen RP, Sheardown SA, Yue L, Burchard EG, Brett CM, Giacomini KM (2008) Effect of genetic variation in the organic cation transporter 1, OCT1, on metformin pharmacokinetics. Clin Pharmacol Ther 83(2):273–280. doi:10.1038/sj.clpt.6100275, 6100275 [pii]
Shu Y, Leabman MK, Feng B, Mangravite LM, Huang CC, Stryke D, Kawamoto M, Johns SJ, DeYoung J, Carlson E, Ferrin TE, Herskowitz I, Giacomini KM (2003) Evolutionary conservation predicts function of variants of the human organic cation transporter, OCT1. Proc Natl Acad Sci U S A 100(10):5902–5907. doi:10.1073/pnas.0730858100, 0730858100 [pii]
Shu Y, Sheardown SA, Brown C, Owen RP, Zhang S, Castro RA, Ianculescu AG, Yue L, Lo JC, Burchard EG, Brett CM, Giacomini KM (2007) Effect of genetic variation in the organic cation transporter 1 (OCT1) on metformin action. J Clin Invest 117(5):1422–1431
Singh SK, Piscitelli CL, Yamashita A, Gouaux E (2008) A competitive inhibitor traps LeuT in an open-to-out conformation. Science 322(5908):1655–1661. doi:10.1126/science.1166777, 322/5908/1655 [pii]
Singh SK, Yamashita A, Gouaux E (2007) Antidepressant binding site in a bacterial homologue of neurotransmitter transporters. Nature 448(7156):952–956
Smith DE, Clemencon B, Hediger MA (2013) Proton-coupled oligopeptide transporter family SLC15: physiological, pharmacological and pathological implications. Mol Aspects Med 34(2–3):323–336. doi:10.1016/j.mam.2012.11.003
Soding J, Biegert A, Lupas AN (2005) The HHpred interactive server for protein homology detection and structure prediction. Nucleic Acids Res 33(Web Server issue):W244–W248. doi:10.1093/nar/gki408
Sonnhammer EL, von Heijne G, Krogh A (1998) A hidden Markov model for predicting transmembrane helices in protein sequences. Proc Int Conf Intell Syst Mol Biol 6:175–182
Soto CS, Fasnacht M, Zhu J, Forrest L, Honig B (2008) Loop modeling: sampling, filtering, and scoring. Proteins 70(3):834–843. doi:10.1002/prot.21612
Sperandio O, Miteva MA, Delfaud F, Villoutreix BO (2006) Receptor-based computational screening of compound databases: the main docking-scoring engines. Curr Protein Pept Sci 7(5):369–393
Stamm M, Staritzbichler R, Khafizov K, Forrest LR (2013) Alignment of helical membrane protein sequences using alignme. PLoS One 8(3):e57731. doi:10.1371/journal.pone.0057731
Traynor K (2013) Canagliflozin approved for type 2 diabetes. Am J Health Syst Pharm 70(10):834. doi:10.2146/news130035
Trott O, Olson AJ (2010) AutoDock Vina: improving the speed and accuracy of docking with a new scoring function, efficient optimization, and multithreading. J Comput Chem 31(2):455–461. doi:10.1002/jcc.21334
Tsirigos KD, Hennerdal A, Kall L, Elofsson A (2012) A guideline to proteome-wide alpha-helical membrane protein topology predictions. Proteomics 12(14):2282–2294. doi:10.1002/pmic.201100495
Tusnady GE, Dosztanyi Z, Simon I (2005) TMDET: web server for detecting transmembrane regions of proteins by using their 3D coordinates. Bioinformatics 21(7):1276–1277. doi:10.1093/bioinformatics/bti121

Vander Heiden MG, Cantley LC, Thompson CB (2009) Understanding the Warburg effect: the metabolic requirements of cell proliferation. Science 324(5930):1029–1033. doi:10.1126/science.1160809

Verdonk ML, Cole JC, Hartshorn MJ, Murray CW, Taylor RD (2003) Improved protein–ligand docking using GOLD. Proteins 52(4):609–623. doi:10.1002/prot.10465

Verrey F, Closs EI, Wagner CA, Palacin M, Endou H, Kanai Y (2004) CATs and HATs: the SLC7 family of amino acid transporters. Pflugers Arch 447(5):532–542. doi:10.1007/s00424-003-1086-z

Wang Y, Welty DF (1996) The simultaneous estimation of the influx and efflux blood–brain barrier permeabilities of gabapentin using a microdialysis-pharmacokinetic approach. Pharm Res 13(3):398–403

Watanabe A, Choe S, Chaptal V, Rosenberg JM, Wright EM, Grabe M, Abramson J (2010) The mechanism of sodium and substrate release from the binding pocket of vSGLT. Nature 468 (7326):988–991. doi:10.1038/nature09580

Weyand S, Shimamura T, Yajima S, Suzuki S, Mirza O, Krusong K, Carpenter EP, Rutherford NG, Hadden JM, O'Reilly J, Ma P, Saidijam M, Patching SG, Hope RJ, Norbertczak HT, Roach PC, Iwata S, Henderson PJ, Cameron AD (2008) Structure and molecular mechanism of a nucleobase-cation-symport-1 family transporter. Science 322(5902):709–713. doi:10.1126/science.1164440, 1164440 [pii]

Wise DR, Thompson CB (2010) Glutamine addiction: a new therapeutic target in cancer. Trends Biochem Sci 35(8):427–433. doi:10.1016/j.tibs.2010.05.003

Xiang Z, Steinbach PJ, Jacobson MP, Friesner RA, Honig B (2007) Prediction of side-chain conformations on protein surfaces. Proteins 66(4):814–823. doi:10.1002/prot.21099

Yamashita A, Singh SK, Kawate T, Jin Y, Gouaux E (2005) Crystal structure of a bacterial homologue of Na^+/Cl^- dependent neurotransmitter transporters. Nature 437(7056):215–223

Yarov-Yarovoy V, Schonbrun J, Baker D (2006) Multipass membrane protein structure prediction using Rosetta. Proteins 62(4):1010–1025. doi:10.1002/prot.20817

Yernool D, Boudker O, Jin Y, Gouaux E (2004) Structure of a glutamate transporter homologue from *Pyrococcus horikoshii*. Nature 431(7010):811–818

Zamek-Gliszczynski MJ, Hoffmaster KA, Tweedie DJ, Giacomini KM, Hillgren KM (2012) Highlights from the international transporter consortium second workshop. Clin Pharmacol Ther 92(5):553–556. doi:10.1038/clpt.2012.126

Zemla A, Venclovas C, Moult J, Fidelis K (1999) Processing and analysis of CASP3 protein structure predictions. Proteins Suppl 3:22–29

Zhao Y, Terry D, Shi L, Weinstein H, Blanchard SC, Javitch JA (2010) Single-molecule dynamics of gating in a neurotransmitter transporter homologue. Nature 465(7295):188–193. doi:10.1038/nature09057

Zhao Y, Terry DS, Shi L, Quick M, Weinstein H, Blanchard SC, Javitch JA (2011) Substrate-modulated gating dynamics in a Na(+)-coupled neurotransmitter transporter homologue. Nature. doi:10.1038/nature09971